J-Researchers

Journal of Civil Engineering Researchers

Journal homepage: www.journals-researchers.com

Damage Identification in Beams and Plates Using Wavelet Theory and Firefly Optimization Algorithm

Saeed Fallahian,[a,*] Seyed Mohammad Seyedpoor,[a] Himan Khodaei[a]

[a] *Department of Civil Engineering, Shomal University, Amol, Iran*

ABSTRACT

The ability to identify structural damage in its earliest stages cannot be overstated in terms of importance. This study uses a two-step procedure based on wavelet theory and an optimization method to identify the location and severity of damage in beams and plates. The damage simulates through the introduction of cracks at targeted locations. Acceleration responses obtained from a dynamic analysis using finite element method undergo wavelet transformation, enabling detailed analysis of the dynamic response signals. Through filtering processes, the structural response signal details are extracted. Disturbances appearing in the signal detail plots indicate the presence of damage, leading to the development of a quantitative index for determining probable damage locations. The second phase is used to properly determine the location and magnitude of the damage using firefly optimization algorithm. To assess the effectiveness of the proposed method, three numerical examples including two beams with 16 and 27 elements, and a plate with different support conditions, one with two-edge fixed supports and another with four-edge fixed supports are considered. Different damage scenarios with noise interferences are considered for the structures. The findings indicate that the proposed methodology shows outstanding results in terms of identifying the location and severity of damage using acceleration responses with considering noise.

ARTICLE INFO

Received: July 19, 2025
Accepted: September 07, 2025

Keywords:
Damage Detection
Wavelet Theory
Optimization
Firefly Algorithm
Beams and Plates

DOI: 10.61186/JCER.7.4.34
DOR: 20.1001.1.22516530.1399.11.4.1.1

1. Introduction

The occurrence of damage during the service life of structures is inevitable and it can be considered one of the main causes of failure in structural systems. Structural damage typically manifests locally in specific members or connections, progressively spreading over time. Failing to detect local damage promptly can lead to a sudden catastrophic failure. Therefore, proper identification of damaged members in structures, along with timely repair and replacement, increases operational life of structures and prevents any probable global damage. Damage causes changes in dynamic and static responses, materials, geometry, and other characteristics of structures. Structural Health Monitoring (SHM) is basically the observation and discovering of such changes in structures during their lifetime, aiming to identify damage. As a result, the health monitoring of structures, either permanently or by periodic testing, can enhance safety, integrity, and proper behavior of structures. Wavelet transforms represent one of the

* Corresponding author. Tel.: + 98 11 2203726; e-mail s.fallahian1@gmail.com.

damage detection methods in structures based on vibration data and signal processing, holding significant importance in damage identification. In recent years, the application of wavelet transforms using vibration responses has garnered much attention for damage detection in structures.

In 2001, Cook et al. successfully identified crack occurrence in beams using Haar and Gabor wavelet functions. Their investigation examined the influence of various crack characteristics including length, orientation, and width, as well as different boundary conditions such as simply supported and fixed supports. The findings demonstrated superior effectiveness of Haar wavelets for identifying discrete cracks [1]. In 2004, Okafor and Swarez conducted health monitoring evaluations on single-story, single-bay beams and frames under static and dynamic loading using discrete and continuous transforms. The damage manifested through disruption and disturbance in structural responses. These disturbances, which remain undetectable through direct structural response analysis, become apparent when evaluated using continuous wavelet transform coefficients or detailed signals from discrete transforms. The results demonstrated highly accurate identification and detection of spatial damage locations [2]. Loutridis et al. (2005) used two-dimensional wavelet transforms in the detection of cracks in plate structures. The crack position and size were well reflected in the transformed response, where the vibration behavior of a cracked plate was transformed into the wavelet domain. Quantitative crack depth estimation was performed using maximum values and energy content of wavelet coefficients. They examined plates with cracks of varying depths and positions. The effects of increased noise on method accuracy were investigated using stress noise testing. The proposed method gained significant attention due to its computational simplicity and high result accuracy [3]. In 2006, Roca and Wilde focused on vibration-based structural damage identification using continuous wavelet transforms. They experimentally tested a plexiglass cantilever beam and a four-edge fixed steel plate. Laboratory-obtained modal shapes from the structures (beams and plates) were analyzed using continuous Gaussian and orthogonal inverse wavelet transforms. The proposed wavelet analysis effectively identified damage locations without prior knowledge of structural characteristics or mathematical models [4]. In 2012, Jiang and Liang evaluated multiple damage in thin plate structures using a two-stage approach. They initially applied two-dimensional wavelet transforms for damage location determination, then assessed damage severity at identified locations using particle swarm optimization algorithms. Subsequently, they examined the relationship between damage severities and natural frequencies through finite element analyses. It has been shown that the suggested approach is properly effective in identifying various damages, despite the fact that natural frequencies could not be accurately determined. In general, the findings showed that there was a good assessment of the damage severities by using natural frequencies [5]. In 2013, Jahangir and Esfahani evaluated damage in reinforced concrete beams using wavelet transforms of biorthogonal vibration modes—normal and inverse—under incremental loading effects. Results provided a suitable index for identifying spatial damage locations in beams through detailed signals from inverse biorthogonal wavelet transforms applied to the first strain mode [6]. In 2014, Ezzaldin et al. presented spatial location identification and crack magnitude determination in beams using discrete wavelet transforms in ANSYS software. The disturbances present in the plots demonstrated increased effects of crack depth relative to crack width [7]. In 2016, Hajizadeh et al. evaluated damage detection methods in plates based on two-dimensional wavelets, utilizing both dynamic responses (modal deformations) and static responses (including rotation, stress, and displacement). The results indicated successful evaluation and detection of cracks in plate structures using both static and dynamic responses [8]. In 2019, Ahmadi et al. conducted the identification and simulation of simply supported steel beams in ABAQUS software through comparative evaluation of analytical results from continuous wavelet transforms under primary and secondary conditions of vibration modal shapes. The interpolated modal shape vectors of beams in healthy and defective states were applied as input for Coiflet5 continuous wavelet transforms in MATLAB software. The results indicated the presence of disturbances and irregularities in wavelet coefficients generated at spatial locations of damage occurrence in secondary wavelet analyses compared to primary analyses [9]. In 2020, Guo et al. introduced a novel method for identifying structural microcracks based on wavelet transforms and an Improved Particle Swarm Optimization (IPSO) algorithm. Initially, the specific characteristics of wavelet coefficients were used to determine damage location in the structure, and subsequently, the IPSO algorithm was employed to determine the severity of structural damage. To evaluate the performance of the proposed method in the research, structural microcrack intensity was considered up to a maximum of 10%, and the structure was examined through numerical simulation and experimental testing under various damage scenarios. The IPSO algorithm was compared to the standard Particle Swarm Optimization, Genetic Algorithm (GA), and Bat Algorithm (BA). Wavelet transforms were very effective in the process of identifying the location of damage, and the IPSO algorithm was more effective in identifying the severity of the structural damage than other main algorithms [10]. In 2023, Luo et al. addressed structural damage identification based on one-dimensional convolutional neural network

groups, considering sensor errors on a simply supported steel bridge. Based on the sensor configuration, several convolutional neural network sub-models were created to extract features from raw vibration data for sensor fault detection and structural damage identification. Subsequently, two convolutional neural network groups—the sensor fault detection group and the damage identification group—were designed based on the performance of each model. The sensor fault detection group determines whether sensor data is abnormal and cuts off abnormal signals. The remaining normal signals enter the damage identification group, and final damage identification results are calculated based on a statistical decision-making module. Results showed that the detection accuracy for sensor faults and damage identification of each model varies at different noise levels, while the accuracy of final damage identification results reaches one hundred percent [11]. In 2024, Abdushkour et al. focused on structural damage identification using wavelet transforms based on signal derivatives. Derivative-Based Wavelet Transform (DBWT) represents one of the innovative approaches in signal analysis that reveals damage-sensitive regions and is utilized to enhance accuracy in damage detection and structural changes. The study addressed the impact of digital signal types on wavelet transform accuracy in engineering applications and presented an efficient wavelet function based on signal derivatives for improving damage detection in beam structures. Consequently, signals obtained from steel beam modal shapes were utilized to evaluate the effectiveness of derivative-based wavelet transforms. They pointed out the relevance of the choice of signal type in improving the accuracy of wavelet transforms in erroneous and damaged signal detection. The outcomes revealed that the use of signal derivatives in wavelet transforms can identify the location of damage with high precision in all the circumstances of damage [12]. In 2025, Zhao et al. presented edge damage detection in structural members using wavelet transforms and Immune-Genetic Algorithm (I-GA). Due to the capability of Wavelet Transform (WT) in identifying damage details in strain modes, the method has attracted considerable attention. Typically, when applying wavelet transforms, damage at structural edges remains ambiguous and undetectable, primarily due to edge effects. To fix this, the analysis is performed carefully at the location of the damage with the help of wavelet transforms by introducing a suitable suffix to the original vibration signal that essentially minimises the edge effects. Besides, an I-GA that integrates a genetic and immune algorithm is utilized to avoid the shortcomings of conventional intelligent algorithms in determining the severity of the damage. The efficiency of this approach for detecting the location of edge damage was validated, and influential parameters, such as the location of damage, noise effects, and damage severity, were measured [13].

In this research a two-stage method based on wavelet theory and optimization method to identify the location and severity of damage to beam and plate structures has been proposed. To identify the location and approximate magnitude of damage in a structure, acceleration responses obtained from a finite element analysis are subjected to wavelet transforms. Subsequently, dynamic response signals are analyzed, and response signal details are extracted using filters. Disturbances in the response signal detail plots indicate the presence of damage. This principle can lead to the introduction of a quantitative index for determining probable damage locations. Then, in the second stage, precisely identifying damage location and magnitude are performed using Firefly Optimization Algorithm. To ensure the effectiveness of the proposed method, two beam structures with different characteristics as well as a plate structure with various support conditions are examined under different damage scenarios. During assessing the method under investigation, the impact of different parameters affecting the efficiency of the method such as, noise effects, number of damaged elements and so on are also studied

2. Finite Element Simulation of structures

2.1. Beams

For beam simulation, the finite element method is employed through coding in the MATLAB software environment. The Newmark method is used to determine acceleration responses. Damage (crack) is simulated as stiffness reduction at specific locations in the beams. Figure 1 shows the triangular variation of stiffness in beam elements [14,15].

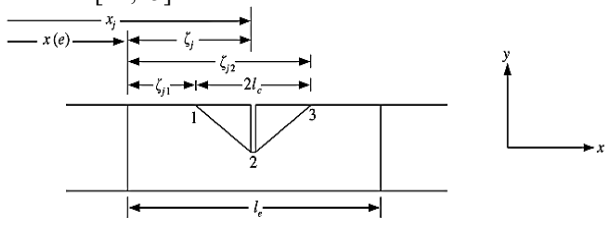

Figure 1. Triangular stiffness variation for crack simulation in different beam elements [14,15]

In this study, crack simulation in beams is performed using stiffness variation with assumptions including: uniform crack depth across the entire beam width and no change in beam mass due to the presence of cracks. Equation (1) represents the flexural stiffness magnitude in the crack region of the beam.

$$EI_e(\xi) = \begin{cases} EI_0 - E(I_0 - I_{cj})\dfrac{(\xi - \xi_{j1})}{(\xi_j - \xi_{j1})} & \text{if } \xi_{j1} \le \xi \le \xi_j \\ EI_0 - E(I_0 - I_{cj})\dfrac{(\xi_{j2} - \xi)}{(\xi_{j2} - \xi_j)} & \text{if } \xi_j \le \xi \le \xi_{j2} \end{cases} \quad (1)$$

$$\xi_{j1} = \xi_j - l_c \quad , \quad \xi_{j2} = \xi_j + l_c$$

$$I_0 = \frac{wd^3}{12} \quad , \quad I_{cj} = \frac{w(d-d_{cj})^3}{12}$$

where the symbols ξ_j, ξ_{j1}, and ξ_{j2}, represent the location of the j-th crack in the e-th element, along with the starting and ending positions of the crack, respectively. The parameters d_{cj}, I_0 and I_{cj} represent the crack depth, the moment of inertia of the intact beam cross-section and the cracked cross-section, respectively. Also, *w* and *d* represent the width and depth of the beam, befor any damage.

Based on definition above, equation (2) can now be used to compute the stiffness matrix of cracked beam element.

$$K_{e.crack} = K_e - K_{cj} \quad (2)$$

where the matrices K_e and K_{cj} represent the stiffness matrix of the intact element and its reduction due to the j-th crack, respectively [14].

2.2. Plates

For simulating plate structures, the finite element method has been employed within the MATLAB software environment. The Newmark method was used to determine acceleration responses. Damage in plates is simulated here as a thickness reduction within an element, as shown in Figure 2. For thin plates, the flexural rigidity is calculated according to equation (3) [5,16].

$$D_0 = \frac{E\,t^3}{12(1-\mu^2)} \quad (3)$$

where E, t, and μ represent elastic modulus, thickness, and Poisson's ratio of the plate, respectively.

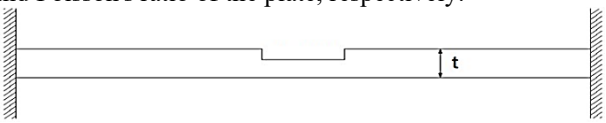

Figure 2. Stiffness variations (thickness reduction) in plates to create damage in different elements [16].

3. Damage Localization Using Wavelet Theory

In recent decades, wavelet transforms have gained widespread application in structural health monitoring and damage detection. These transforms are based on time-frequency analyses and convert signals into small wavelets. Generally, mathematical transformations are applied to signals to extract hidden data within them. Wavelet transforms perform localized regional analyses through large-scale signals, thus possessing the capability to execute local analyses. Wavelet transforms have the ability to perform localized analyses on signals. Through wavelet transforms, signals appear as peaks at discontinuity locations. Furthermore, using wavelet transforms in structures, damage locations are detected as peak locations and disturbances on the graph of base or mother wavelet coefficients. In fact, wavelet analyses have the ability to detect and identify spatial locations of very small damage and discontinuities. In wavelet analyses, the factors used are obtained directly from the time history response of systems using simple tools, and these factors, unlike modal domain-based methods, do not require modal analysis and extraction of natural frequencies of the system and operate independently of them. This means that wavelet analysis is a powerful method that can extract important information from structural response without requiring modal analysis to be performed first. This feature can be a major advantage in some cases, as modal analysis may be time-consuming and complex. In this study, Symlet wavelet functions have been used to identify damage in the structures under investigation, and the structural response used is acceleration. A wavelet is an oscillatory function with a real, periodic, or complex nature with an average value of zero and finite length. Generally, changes in size, location, and final shape of the mother (generator) wavelet function occur through translation and scaling in the signal application range according to equation (4) [17,18].

$$\psi_{u,s}(x) = \frac{1}{\sqrt{s}}\psi\left(\frac{x-u}{s}\right) \quad (4)$$

$$\psi(x) \in L^2(R)$$

where $\psi_{u,s}(x)$, $\psi(x)$, and $L^2(R)$ represent continuous wavelet functions, mother function, and Hilbert space with the capability of measuring square-integrable functions, respectively. Also, the parameters s and u in equation (4), which are real numbers, represent the scaling factor (scale characteristic) and translation (temporal, spatial positions, or center of influence) of wavelets, respectively. For the signal of interest, continuous wavelet transforms are shown in equation (5).

$$w\,f(u,s) = [f,\ \psi_{u,s}] = \frac{1}{\sqrt{s}}\int_{-\infty}^{+\infty} f(x)\,\psi\left(\frac{x-u}{s}\right)dx \quad (5)$$

$$f(x) \in L^2(R)$$

where $w\,f(u,s)$ is the wavelet coefficients of the function $\psi_{u,s}(x)$, and x is the spatial coordinate. Computing and measuring these wavelet coefficients will allow us to capture the variations of the signal in the neighborhood of parameter u, which is proportional to the scaling factor s.

In this research, the structures under investigation are modeled using the finite element method in MATLAB software. Mass and stiffness matrices are formed, and

dynamic responses are computed. The applied load takes the form of a trapezoidal impact, and acceleration responses are determined using the Newmark method. Subsequently, the acceleration responses obtained from a dynamic analysis via finite element method undergo wavelet transformation for dynamic response signal analysis. Through filtering, detailed characteristics of the structural response signal are extracted. In such signals, it can be seen that the occurrence of the irregularities and the peak areas can be used to estimate which areas might be damaged, and the appropriate damage indices can be set. Disturbances in the detailed response signal plots indicate structural damage, leading to the introduction of a wavelet index for identifying probable damage locations.

4. Damage Localization and Quantification Using an Optimization Method

The optimization problem formulation for damage identification in structures can be given in equation (6) [15]:

$$\begin{aligned} &\text{Find: } X^T = \{X_1, X_2, \dots, X_n\} \\ &\text{Minimize: } W(X) \\ &X^T \le X_i \le X^u \end{aligned} \tag{6}$$

where X, X^T, and X^u represent the damage variable vector containing unknown damage location and severity, and the upper and lower bounds of the damage vector, respectively. The variable W represents the objective function, which constitutes one of the most critical components of an optimization problem and serves as a criterion for calculating convergence values and determining algorithm termination. The objective function in this paper is according to equation (7) and it is needed to be minimized [15].

$$W(X) = -\frac{1}{2}\left[\frac{|\Delta R^T.\delta R(X)|^2}{(\Delta R^T.\Delta R)(\delta R(X)^T.\delta R(X))} + \frac{1}{n_p}\sum_{i=1}^{n_p}\frac{\min(R_{x,i}, R_{di})}{\max(R_{x,i}, R_{di})}\right] \tag{7}$$

where R_{di} and R_{xi} represent the i-th components of the response vector in the damaged state R_d and the numerical model response vector R_x, respectively, the vectors ΔR and δR(X) represent the structural response changes relative to the healthy state under damage occurrence and those derived from the numerical model, respectively. Also, n_p is the number of elements in the structural response vector [15]. The response considered in this research is the nodal acceleration, and the firefly algorithm is used to perform the optimization task [19]. Because the main part of the damage identification procedure is the first part, therefore any optimization algorithm can be emplyed here without having an important effect on the performance of the whole method.

5. Numerical Examples

In order to assess the performance of the proposed method, two beams with different properties and elements of 16 and 27 and a plate with two different support conditions of two-sided and four-sided fixed are considered. Damage in beams is defined as a crack on the desired elements according to Sinha et al. [14] and Yazdanpanah and Seydpoor [15], while for plates, damage is simulated using stiffness reduction based on Jiang and Liang [5]. The process entails the modeling of the target structures using finite element method in MATLAB, the construction of mass and stiffness matrices and followed by extracting the dynamic responses, such as natural frequencies, modal deformations and acceleration responses. The loads applied have a short-term non-periodic type of impact, which is in the shape of a trapezoidal force, as shown in Figure 3. The acceleration responses obtained from dynamic analysis undergo wavelet transformations, followed by dynamic response signal analysis. Through filtering, detailed characteristics of the structural response signal are extracted. Disturbances in the detailed structural signal plots indicate the damage presence within the structure. High values of the wavelet index within a specific time window indicate sudden and significant changes in the acceleration response signal during that time interval, which may result from damage occurrence. After damage localization, the firefly algorithm is employed to accurately determine damage locations within structures as well as damage severity. The best values for optimization parameters have been chosen according to Ref. [19] and the optimization will stop if there is no significant improvement in the objective function for a few successive iterations.

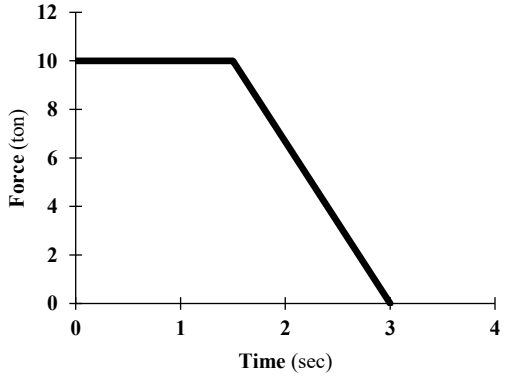

Figure 3 - Applied Force Diagram for Structural Loading

5.1. Sixteen-Element Cantilever Beam

A sixteen-element aluminum cantilever beam with seventeen nodes with two degrees of freedom per node serves as the first example. The boundary conditions of the beam include the translational as well as the rotational springs as shown in Figure 4. The dimensions of the beam are 996 mm, 50 mm and 25 mm in length, width, and depth, respectively and the material properties are Youngs modulus 69.79 GN/m^3, density 2600 kg/m^3, Poisons ratio 0.33, translational spring stiffness (Kt) 26.50 MN/m and rotational spring stiffness (Ktheta) 150 kNm/rad. The beam is initially modeled in MATLAB software, then subjected to a short-term, non-periodic trapezoidal impact load as shown in Figure 3. Dynamic acceleration responses are obtained, and damage identification results are presented through graphical representations. Figure 4 illustrates the finite element model of the beam with a single crack located at the center of element 5 positioned 275 mm from the beam's left end. Table 1 lists three scenarios of damage undertaken in the beam.

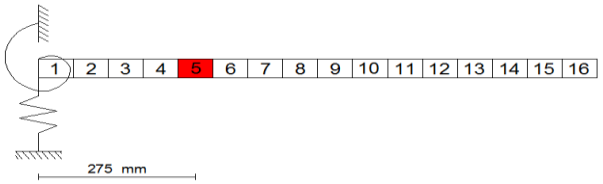

Figure 4. Finite Element Model of Sixteen-Element Cantilever Beam (Red-colored element indicates crack location)

Table 1:
Damage Conditions at 275 mm Position from Beam Left end (Element 5)

Damage Case	Crack depth (mm)	Crack Depth to Beam Depth
First	4	0.16
Second	8	0.32
Third	12	0.48

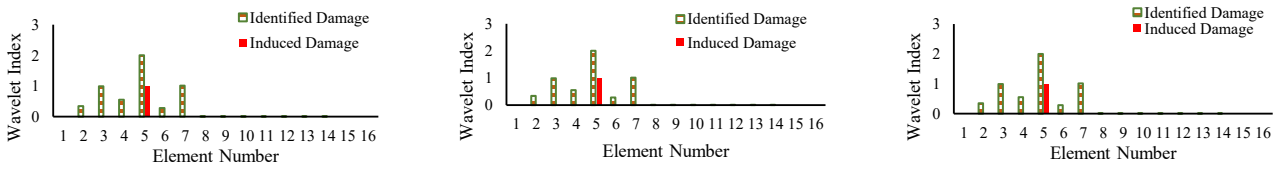

Figure 5. Damage Location for Different Damage States Using Wavelet Index Under Noise-Free Condition

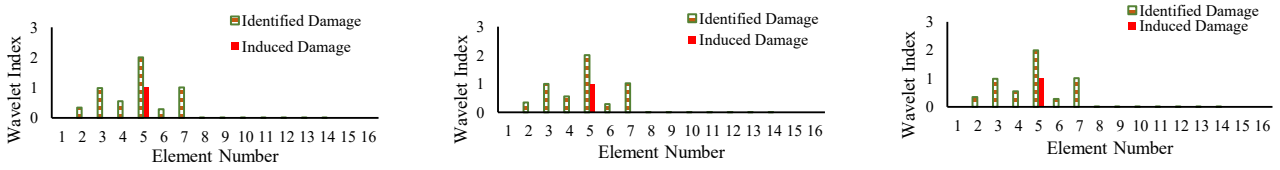

Figure 6. Damage Location for Different Damage States Using Wavelet Index Under 3% Noise Condition

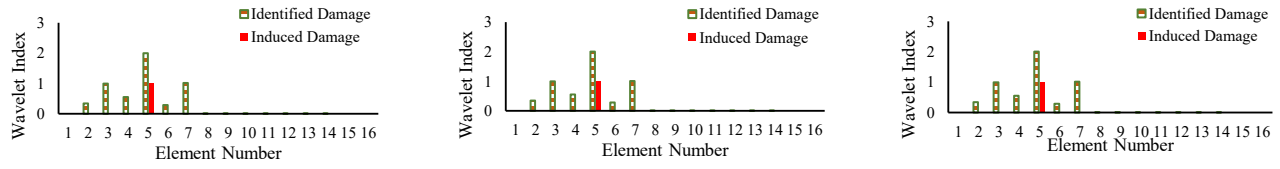

Figure 7. Damage Location for Different Damage States Using Wavelet Index Under 5% Noise Condition

The beam undergoes under the specified damage conditions with and without considering 3% and 5% noise levels. Figures 5, 6, and 7, respectively, demonstrate damage location assessment for different damage states using the wavelet index applied to acceleration responses under noise-free condition and with 3% and 5% noise

considerations. Figures 8, 9, and 10, respectively, show the damage location and severity identification in the second step for various damage cases of the beam under noise-free condition and with 3% and 5% noise considerations.

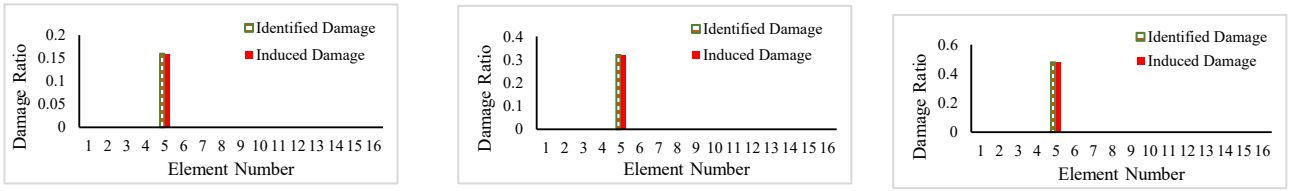

First Damage State Second Damage State Third Damage State

Figure 8. Location and Damage Severity for Different Damage States Under Noise-Free Condition

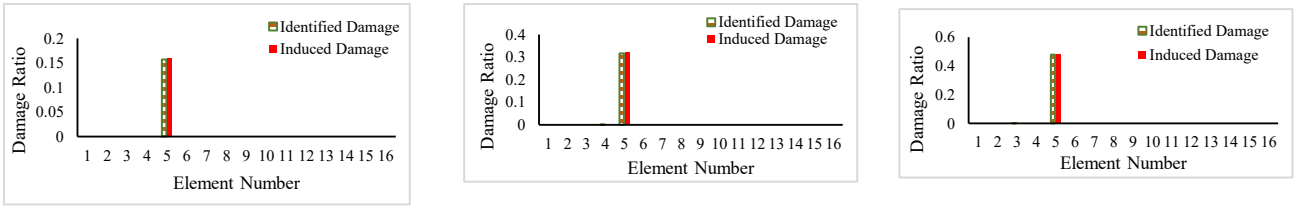

First Damage State Second Damage State Third Damage State

Figure 9. Location and Damage Severity for Different Damage States Under 3% Noise Condition

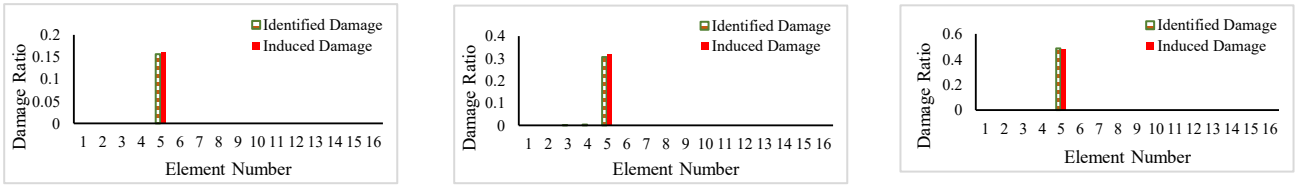

First Damage State Second Damage State Third Damage State

Figure 10. Location and Damage Severity for Different Damage States Under 5% Noise Condition

Considering the damage identification charts for the sixteen-element cantilever beam, the probable damage location (element 5) is effectively detected by the wavelet index regardless of whether noise is present in the data. This method demonstrates excellent capability in identifying both damage location and severity with high precision. The detection results of damage severity compared to precise values under 3% and 5% noise are listed in Table 2.

5.2. Twenty-Seven Element Simply Supported Beam

A twenty-seven-element aluminum simply supported beam with twenty-eight nodes, having two degrees of freedom per node, considered as the second example. The beam dimensions include length, width, and depth of 1832mm, 50mm, and 25mm, respectively, with Young's modulus of 69.79 GN/m², density of 2600 kg/m³, and Poisson's ratio of 0.33. The beam finite element model with a single crack at element 9 (position is 595mm off the origin) and two cracks at elements 9 and 12 (position is 595mm and 800mm off the beam origin) are shown in Figure 11a and b, respectively. Damage conditions including single and double damage cases are shown in Table 3.

The beam was evaluated under the specified damage conditions, both with noise free, 3% and 5% noise considerations. Figures 12 to 17, respectively, show damage location assessment for various single and double damage conditions using the wavelet index on acceleration responses under noise-free and noisy conditions (3% and 5% noise).

Table 2
Error Rate of identifying Damage severity for Different Cases Under 3% and 5% Noise

Noise (%)	Damage Case	Actual Damage Severity (%)	Error Rate (%)
3%	First	16	1.75
	Second	32	1.16
	Third	48	0.30
5%	First	16	2.03
	Second	32	4.15
	Third	48	1.19

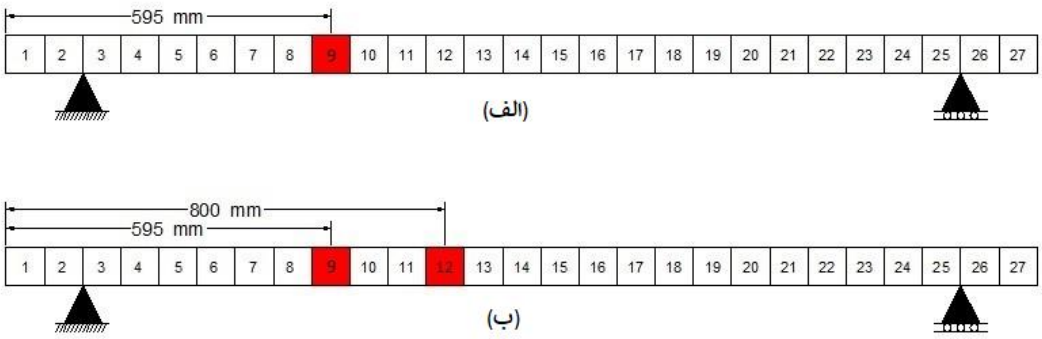

Figure 11. Finite Element Model of a Twenty-Seven Element Simply Supported Beam (a) Single damaged element and (b) Two damaged elements (Red elements indicate crack locations)

Table 3

Different Damage Conditions of twenty-seven-element simply supported beam

Damage Condition	Damage Case	Damaged Element	Crack depth (mm)	Crack depth to Beam Depth
Single Damage	First	9	4	0.16
	Second	9	8	0.32
	Third	9	12	0.48
Double Damage	First	9	12	0.48
		12	4	0.16
	Second	9	12	0.48
		12	8	0.32
	Third	9	12	0.48
		12	12	0.48

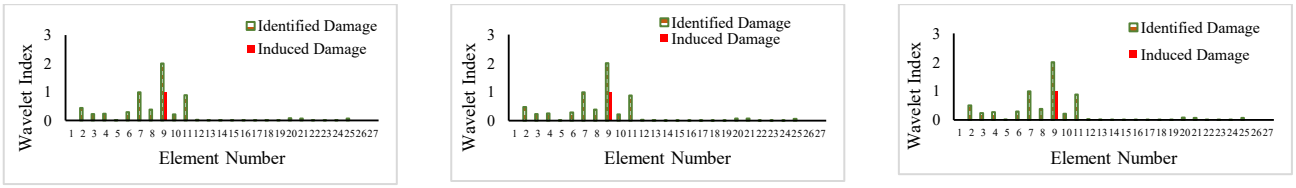

Figure 12. Location for single damage condition under various damage cases using wavelet index without noise

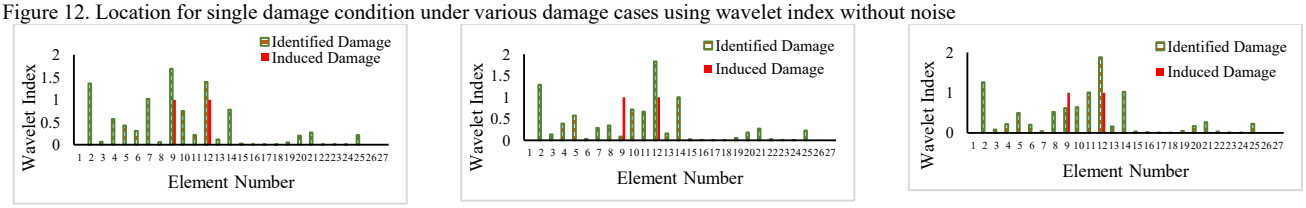

First failure state Second failure state Third failure state

Figure 13. Location for double damage condition under various damage cases using wavelet index without noise

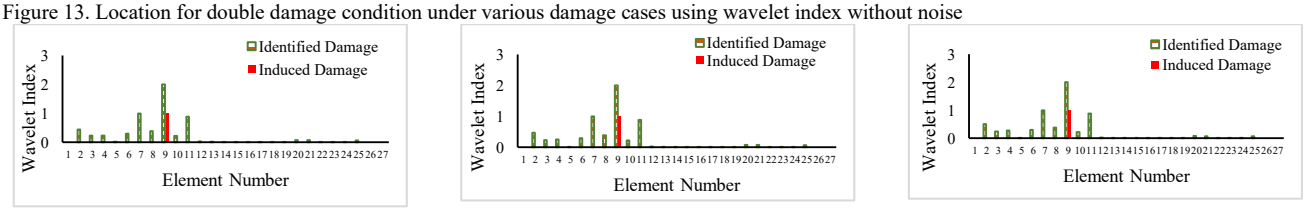

First failure state Second failure state Third failure state

Figure 14. Location for single damage condition under various damage cases using wavelet index with 3% noise

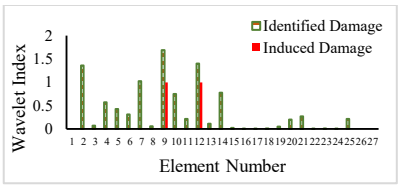

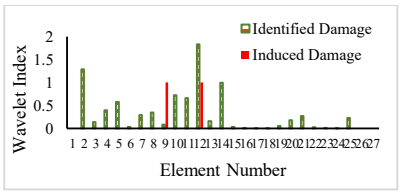

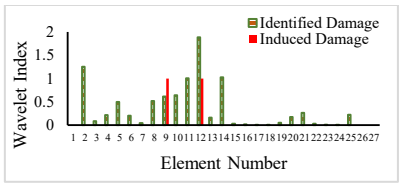

First failure state Second failure state Third failure state

Figure 15. Location for double damage condition under various damage cases using wavelet index with 3% noise

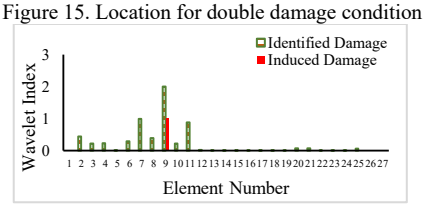

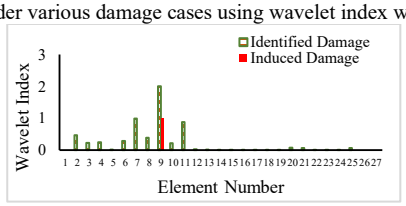

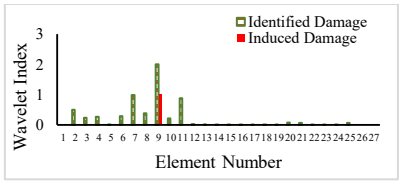

First failure state Second failure state Third failure state

Figure 16. Location for single damage condition under various damage cases using wavelet index with 5% noise

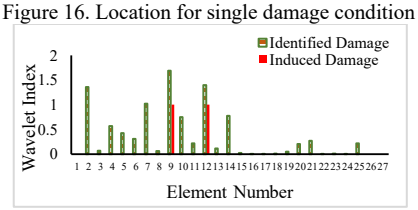

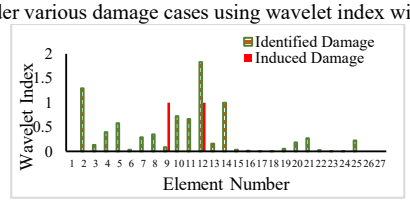

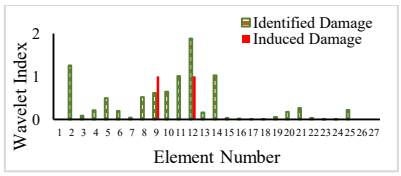

First failure state Second failure state Third failure state

Figure 17. Location for double damage condition under various damage cases using wavelet index with 5% noise

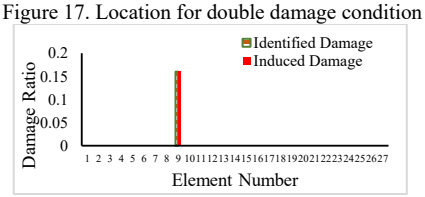

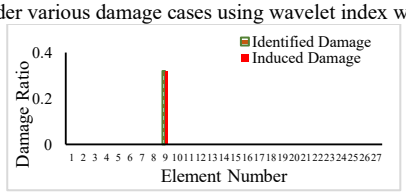

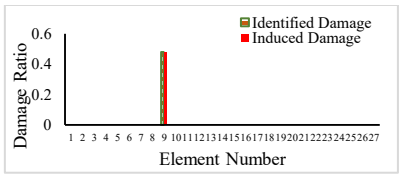

First failure state Second failure state Third failure state

Figure 18. Damage location and severity for single damage condition under various cases without noise

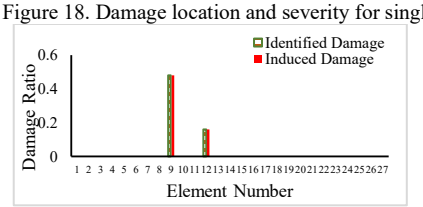

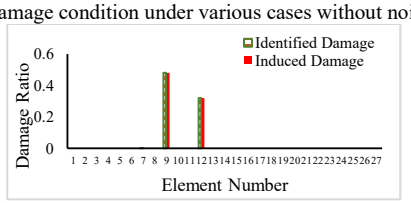

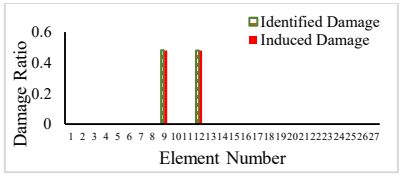

First failure state Second failure state Third failure state

Figure 19. Damage Location and severity for double damage condition under various cases without noise

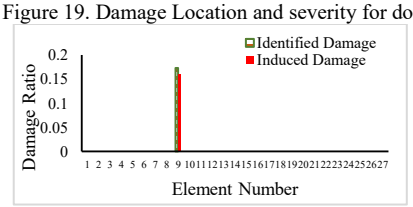

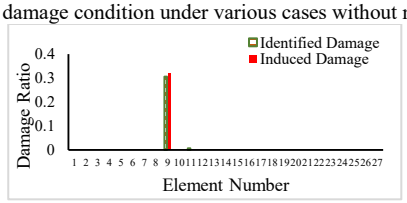

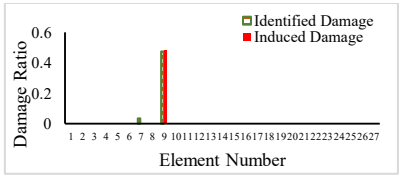

First failure state Second failure state Third failure state

Figure 20. Damage Location and severity for single damage condition under various cases with 3% noise

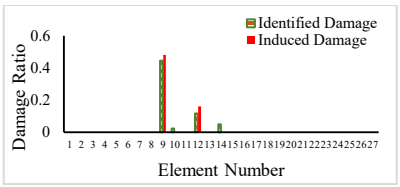

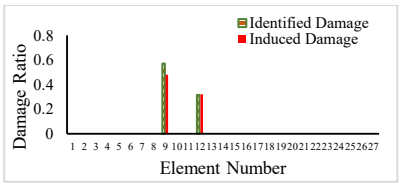

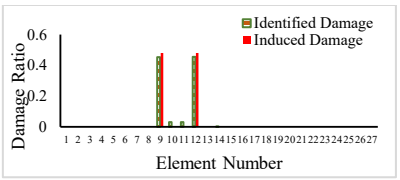

First failure state Second failure state Third failure state

Figure 21. Damage Location and severity for double damage condition under various cases with 3% noise

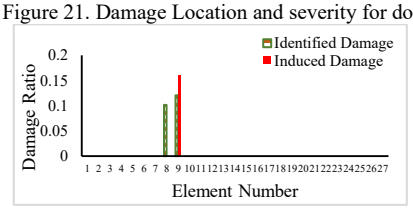

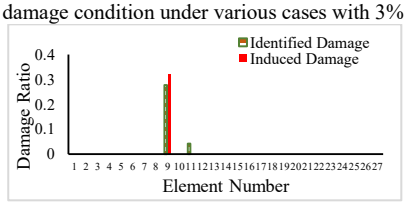

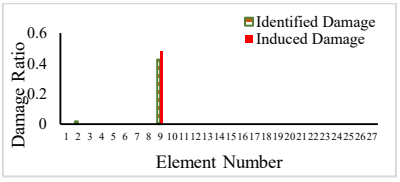

First failure state Second failure state Third failure state

Figure 22. Damage Location and severity for single damage condition under various cases with 5% noise

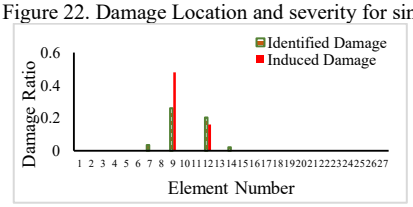

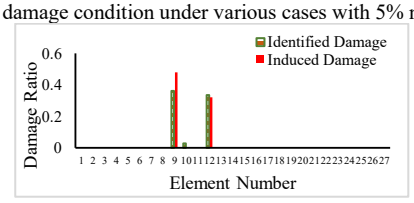

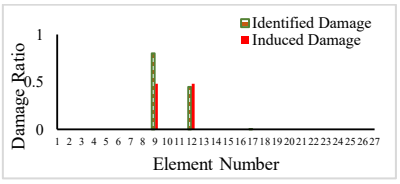

First failure state Second failure state Third failure state

Figure 23. Damage Location and severity for double damage condition under various cases with 5% noise

Table 4
Error Rate of identifying Damage severity for Different Cases Under 3% and 5% Noise

Damage Condition	Damage Case	Actual Damage Severity (%)	Error Rate (%) (Noise 3%)	Error Rate (%) (Noise 5%)
Single Damage	First	16	8.14	24.46
	Second	32	4.55	13.34
	Third	48	1.28	11.49
Double Damage	First	48	7.17	45.66
		16	27.07	26.91
	Second	48	19.06	24.63
		32	1.09	4.91
	Third	48	5.69	66.66
		48	5.11	6.8

Figures 18 through 23 demonstrate damage location and severity identification in the second step for various damage.

According to the damage identification charts for the twenty-seven-element simply supported beam under both single and double damage conditions, the probable damage locations are successfully detected by the wavelet index. For both single and double damage cases, the method demonstrates excellent capability in identifying both damage location and severity with high accuracy, regardless of noise presence in the data. The detection results of damage severity compared to their exact values are given in Table 4.

5.3. Plate with Different Support Conditions

A square plate with dimensions of 560×560 mm and different support conditions including two-edge and four-edge clamped are considered as third example. Each plate edge is divided into 28 elements, resulting in a mesh configuration of 28×28 elements. The plates are 2 mm thick, comprise 841 nodes, and possess 784 elements whose dimensions are 20 mm. The plates have the Young modulus of 200 GPa, a density of 7850 kg/m³ and the Poisson ratio of 0.3. The plates subjected to the trapezoidal impact loading are modeled using MATLAB. Acceleration responses are obtained, and damage identification results

are presented graphically. Damage in the plates includes four different scenarios, with each damage scenario comprising sixteen elements (4×4 configuration). Each damage scenario includes four different thickness reduction values according to Table 5. The length and width of each damage area (sum of four elements in each direction) are 80 mm.

Table 5
Damage Cases in Four Scenarios for Two-Edge and Four-Edge Clamped Plates

Damage Case	Thickness Reduction (mm)	Thickness Reduction (%)	Remaining thickness (mm)
1	0.5	25	1.5
2	1.0	50	1.0
2	1.5	75	0.5
4	1.75	87.5	0.25

Damage locations for scenarios 1 to 4 in the two-edge and four-edge clamped plates are shown in Figures 24 and 25, respectively.

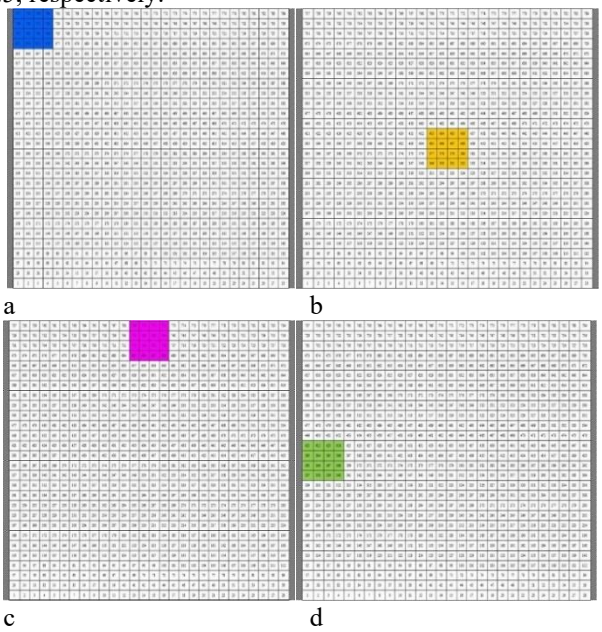

Figure 24. Damage Locations in Scenarios: (a) First, (b) Second, (c) Third, and (d) Fourth for a two-edge clamped plate

Figures 26 to 33 show damage location detection for scenarios 1 to 4 with damage severities of 25%, 50%, 75%, and 87.5% using wavelet analysis without noise consideration for both two-edge and four-edge clamped plates, respectively. Figures 34 to 41, respectively, show damage location assessment for scenarios 1 to 4 with damage severities of 25%, 50%, 75%, and 87.5% for both two-edge and four-edge clamped plates using wavelet analysis with 3% noise applied.

Figures 42 through 49 demonstrate location and severity identification in the second step for scenarios one through four with damage severities of 25%, 50%, 75%, and 87.5% for both two-edge and four-edge clamped plates without noise consideration. Figures 50 through 57 demonstrate location and severity identification in the second step for scenarios one through four with damage severities of 25%, 50%, 75%, and 87.5% for both two-edge and four-edge clamped plates with 3% noise applied.

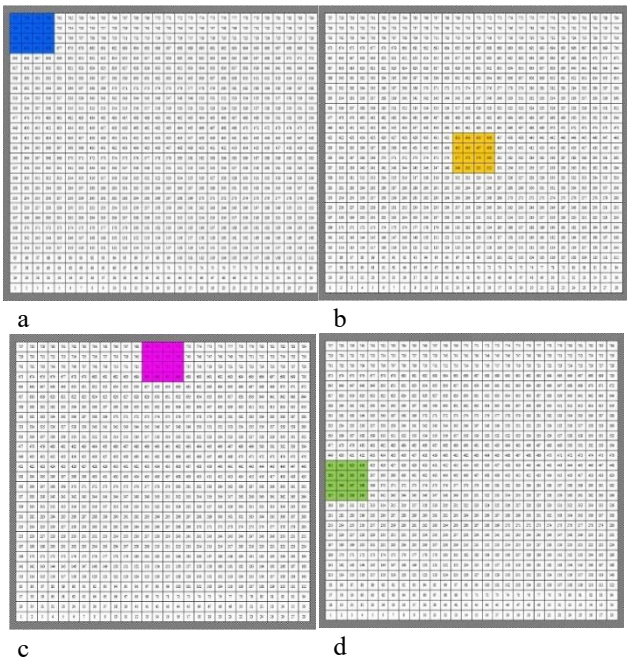

Figure 25. Damage Locations in Scenarios: (a) First, (b) Second, (c) Third, and (d) Fourth for a four-edge clamped plate

As evident from the diagrams, damage location identification in cases with and without noise consideration for both two and four edge clamped plates demonstrates acceptable accuracy. In the 25% damage condition, without considering noise and in scenarios 1 to 4, damage intensity in two edge clamped plates is obtained with differences of 0%, 2.9%, 6.8%, and 8%, respectively, while in four edge clamped plates, the differences were 3.7%, 2.8%, 3.8%, and 12.72%, respectively. In the 50% damage condition, without noise application and in scenarios 1 to 4, damage intensity for two edge clamped plates is evaluated with differences of 4%, 0%, 8.1%, and 15.8%, respectively, while in plates with other boundry conditions, the differences are 19.4%, 5.8%, 14%, and 23.75%, respectively. In the 75% damage condition, without noise application and in scenarios 1 to 4, damage intensity in two edge clamped is evaluated with differences of 0%, 1.3%, 2.7%, and 6.4%, respectively, while in plates clamped on four sides, the differences were 0%, 2.53%, 1.33%, and 0%, respectively. In the 87.5% damage condition, without noise application and in scenarios 1 to 4, damage intensity in simply supported plates on two sides is evaluated with differences of 0%, 1.7%, 1.7%, and 2.3%, respectively, while in plates clamped on four sides, the differences were 0.57%, 3.7%, 1.71%, and 0.57%, respectively.

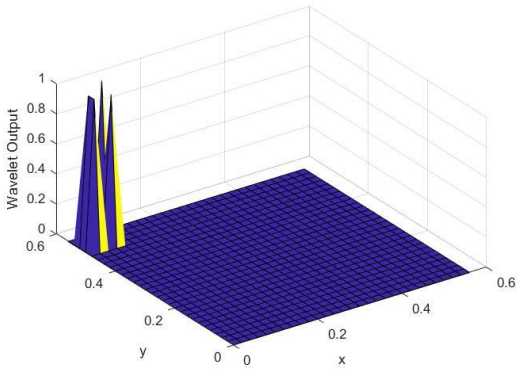

a

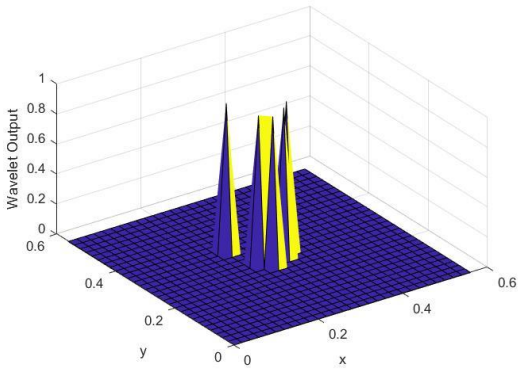

b

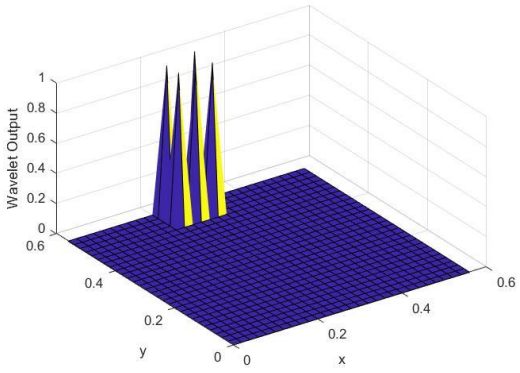

c

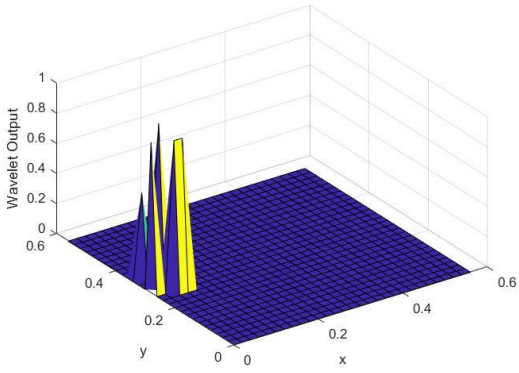

d

Figure 26. Damage localization in scenarios (a) first, (b) second, (c) third, and (d) fourth with 25% damage severity in two-edge clamped plate using wavelet analysis without considering noise

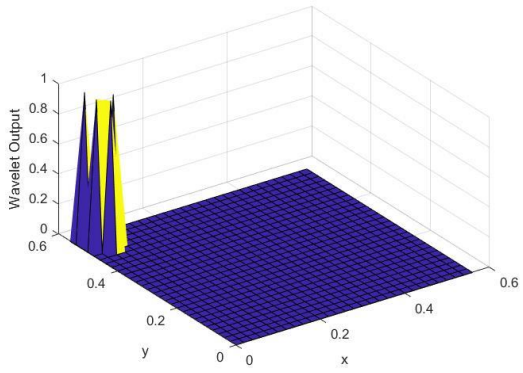

a

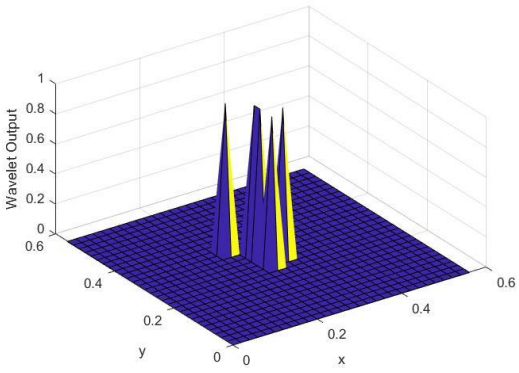

b

Figure 27. Continued on next page

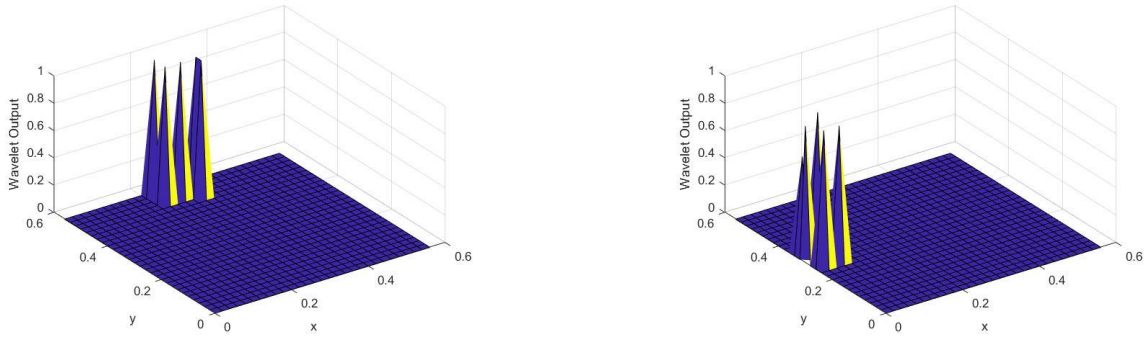

c d

Figure 27. Damage localization in scenarios (a) first, (b) second, (c) third, and (d) fourth with 50% damage severity in two-edge clamped plate using wavelet analysis without considering noise

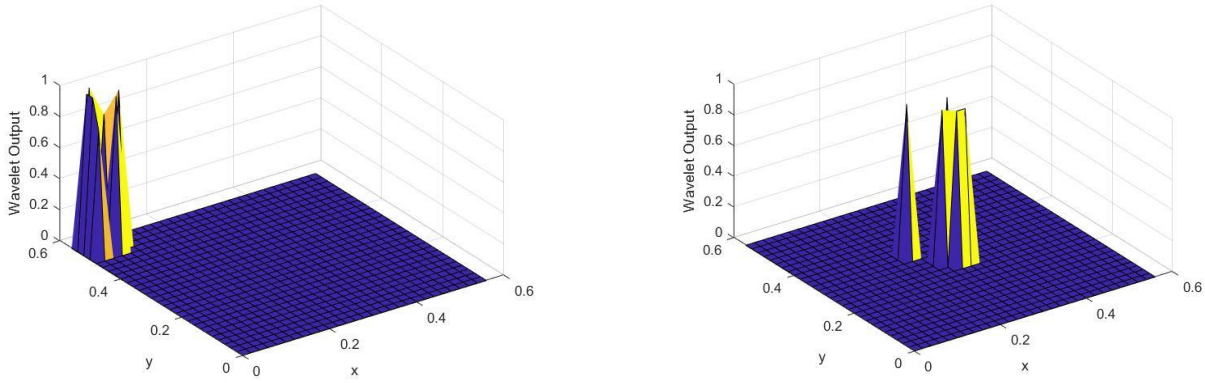

a b

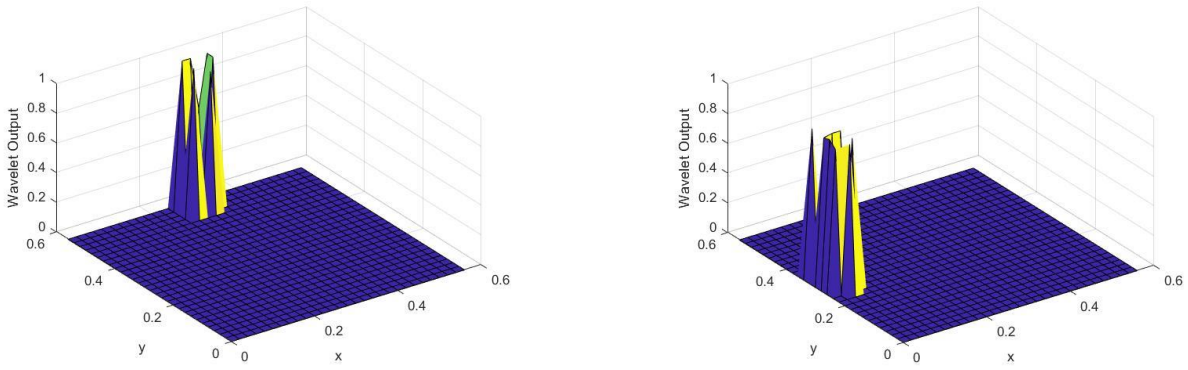

c d

Figure 28. Damage localization in scenarios (a) first, (b) second, (c) third, and (d) fourth with 75% damage severity in two-edge clamped plate using wavelet analysis without considering noise

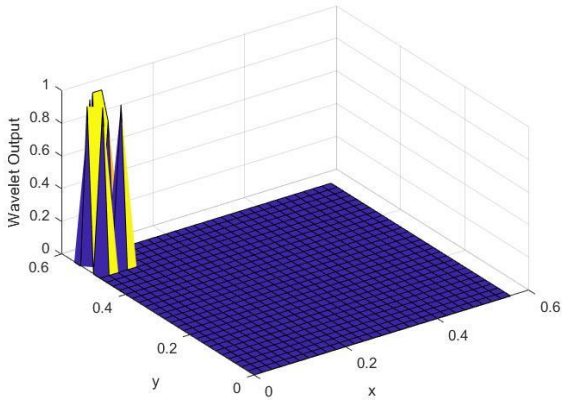

a

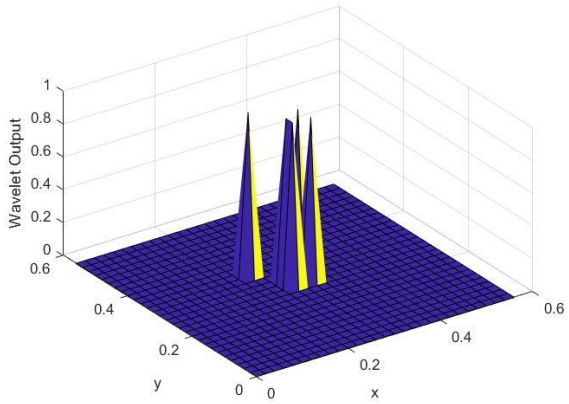

b

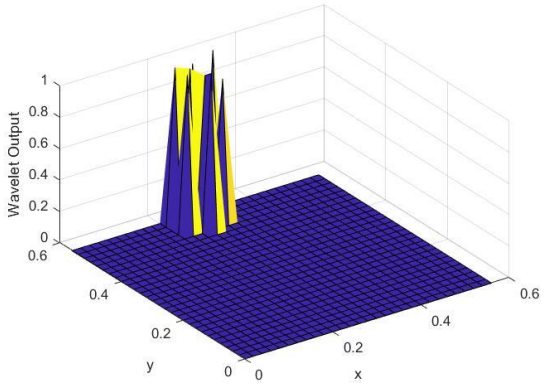

c

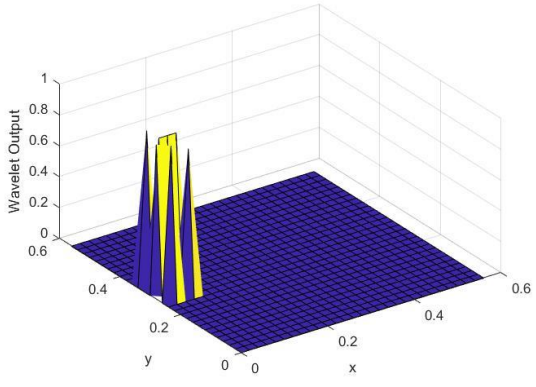

d

Figure 29. Damage localization results for scenarios a) first, b) second, c) third, and d) fourth, with 87.5% damage severity in two-edge clamped plates using wavelet analysis without considering noise

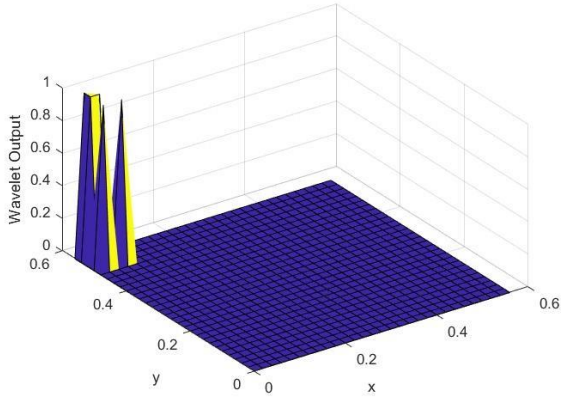

a

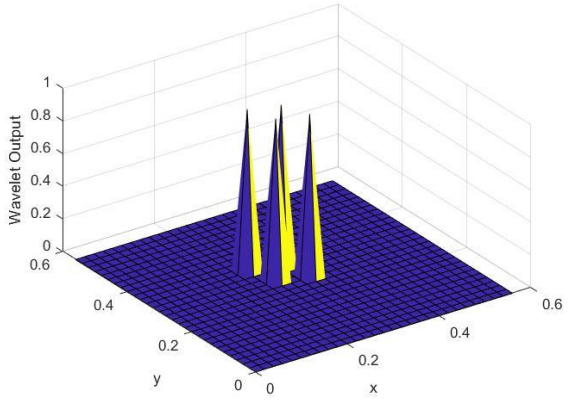

b

Figure 30. Continued on next page

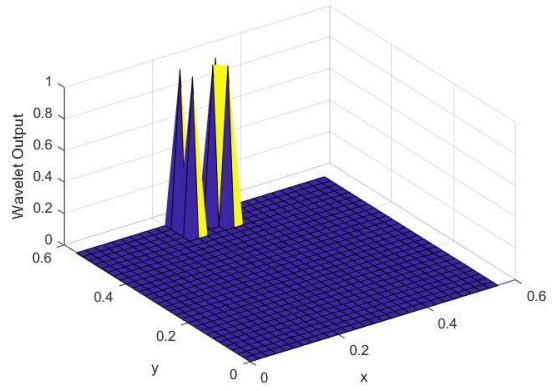

c

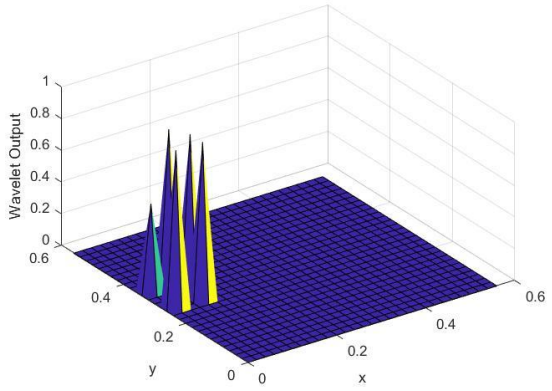

d

Figure 30. Damage localization results for scenarios a) first, b) second, c) third, and d) fourth with 25% damage severity in four-edge clamped plates using wavelet analysis without considering noise

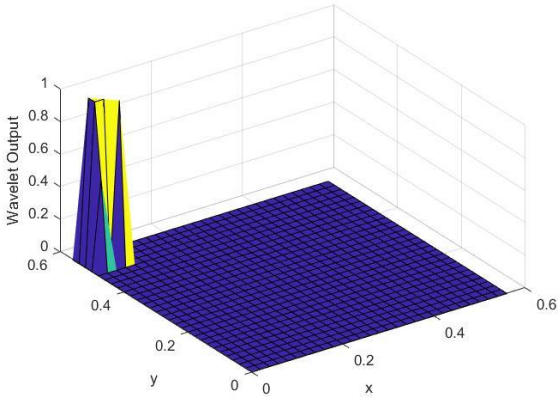

a

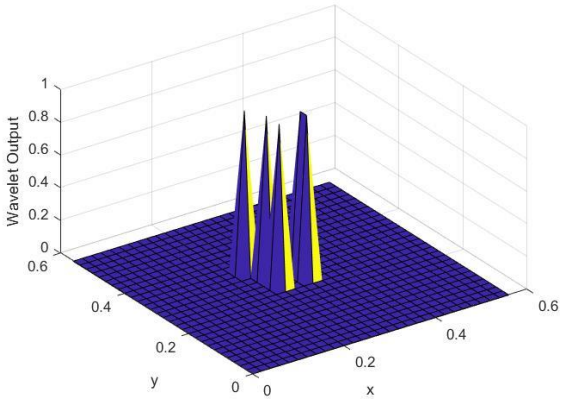

b

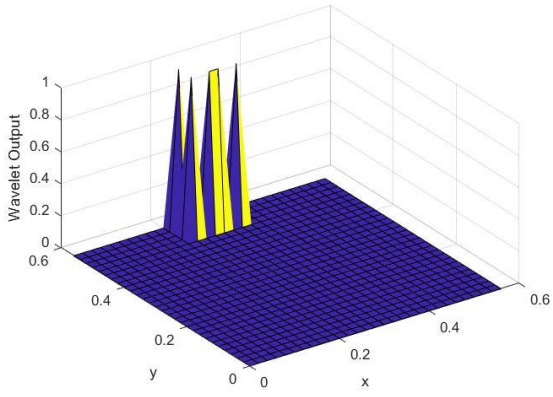

c

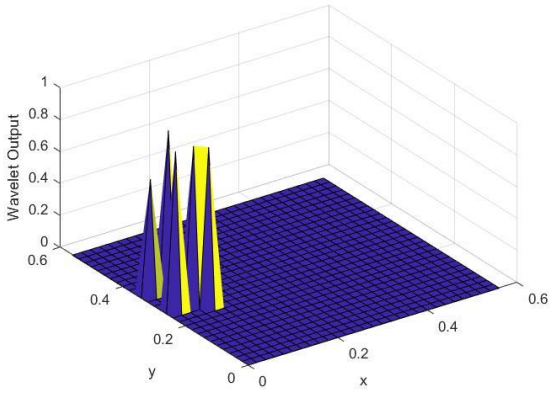

d

Figure 31. Damage localization results for scenarios a) first, b) second, c) third, and d) fourth with 50% damage severity in four-edge clamped plates using wavelet analysis without considering noise

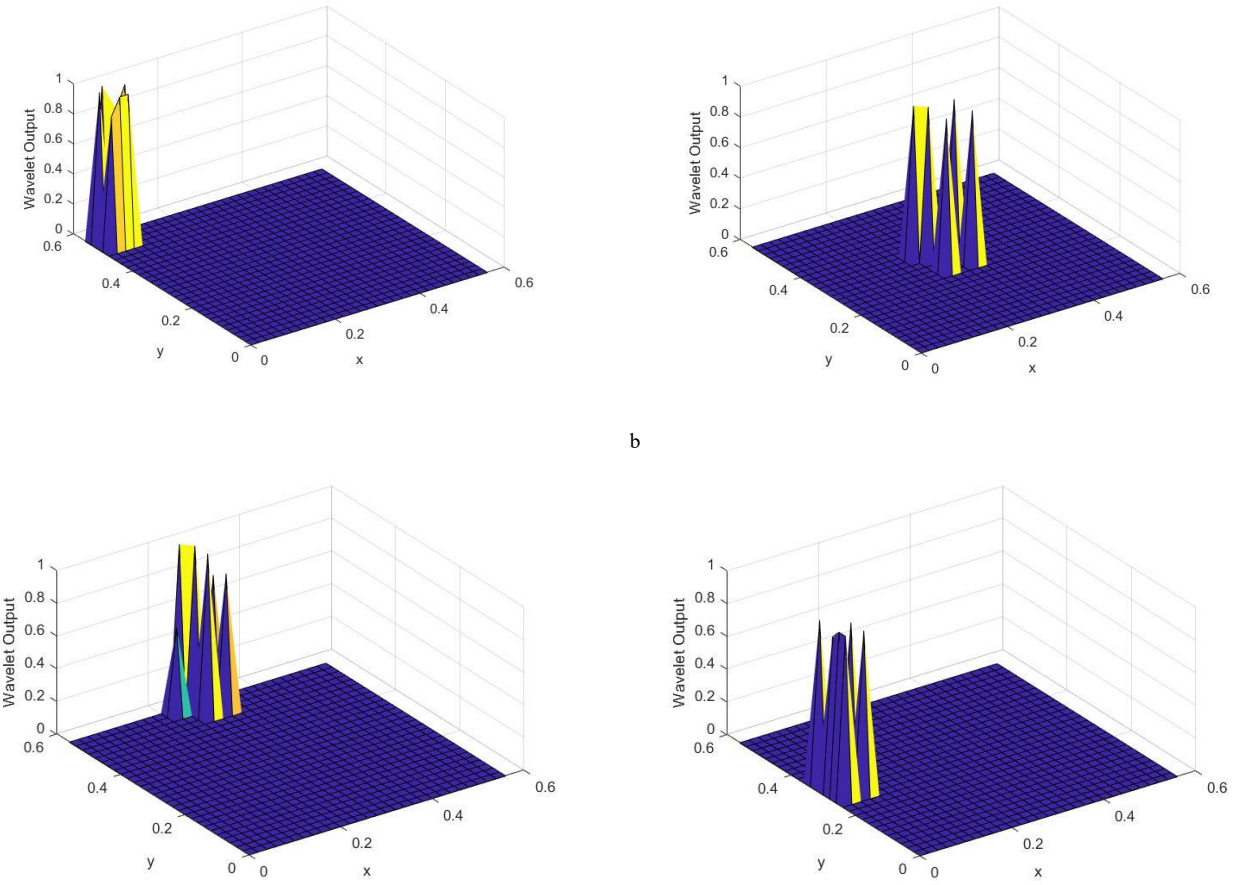

Figure 32. Damage localization results for scenarios a) first, b) second, c) third, and d) fourth with 75% damage severity in four-edge clamped plates using wavelet analysis without considering noise

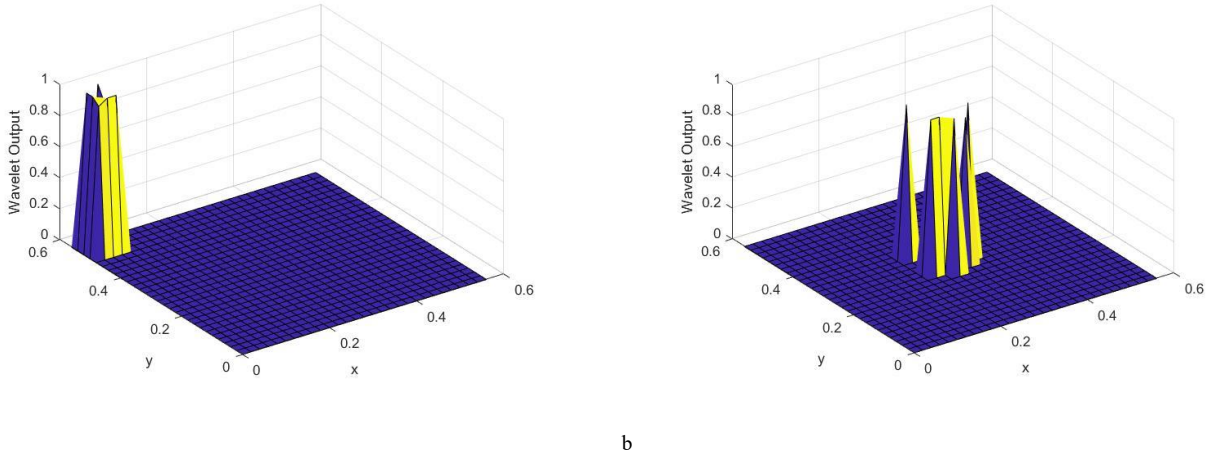

Figure 33. Continued on next page

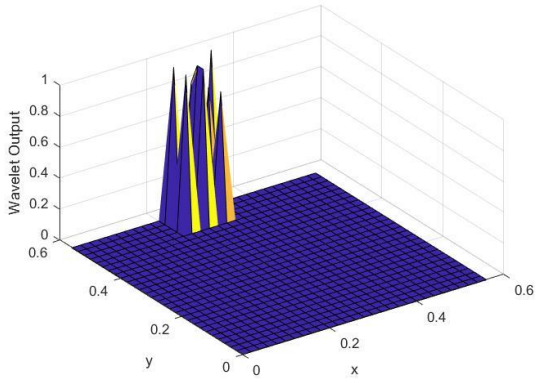

c

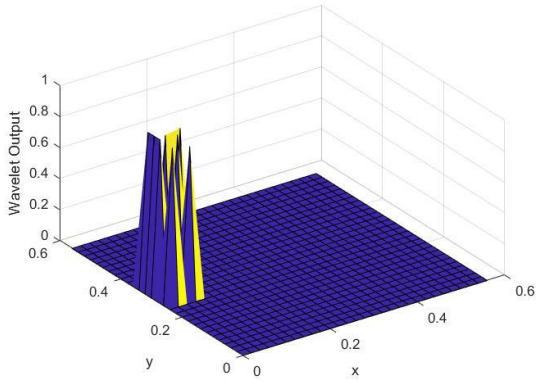

d

Figure 33. Damage localization results for scenarios a) first, b) second, c) third, and d) fourth, with 87.5% damage severity in four-edge clamped plates using wavelet analysis without considering noise

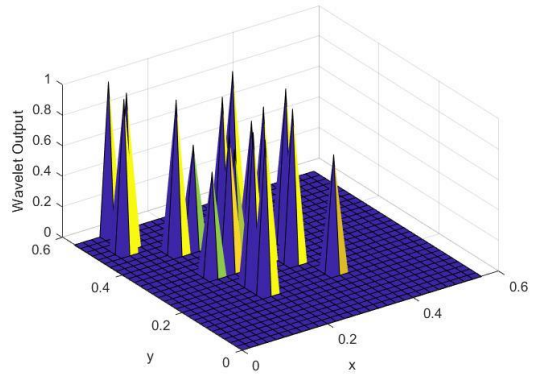

a

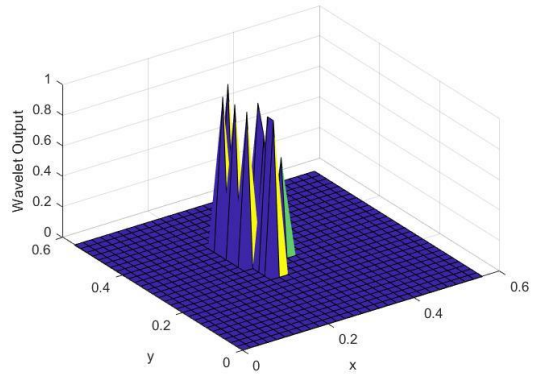

b

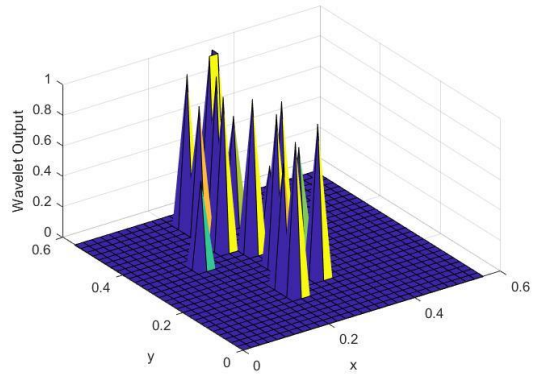

c

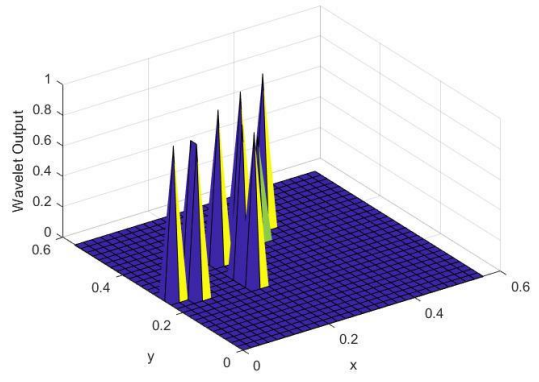

d

Figure 34. Damage localization results for scenarios a) first, b) second, c) third, and d) fourth with 25% damage severity in two-edge clamped plates using wavelet analysis with considering 3% noise

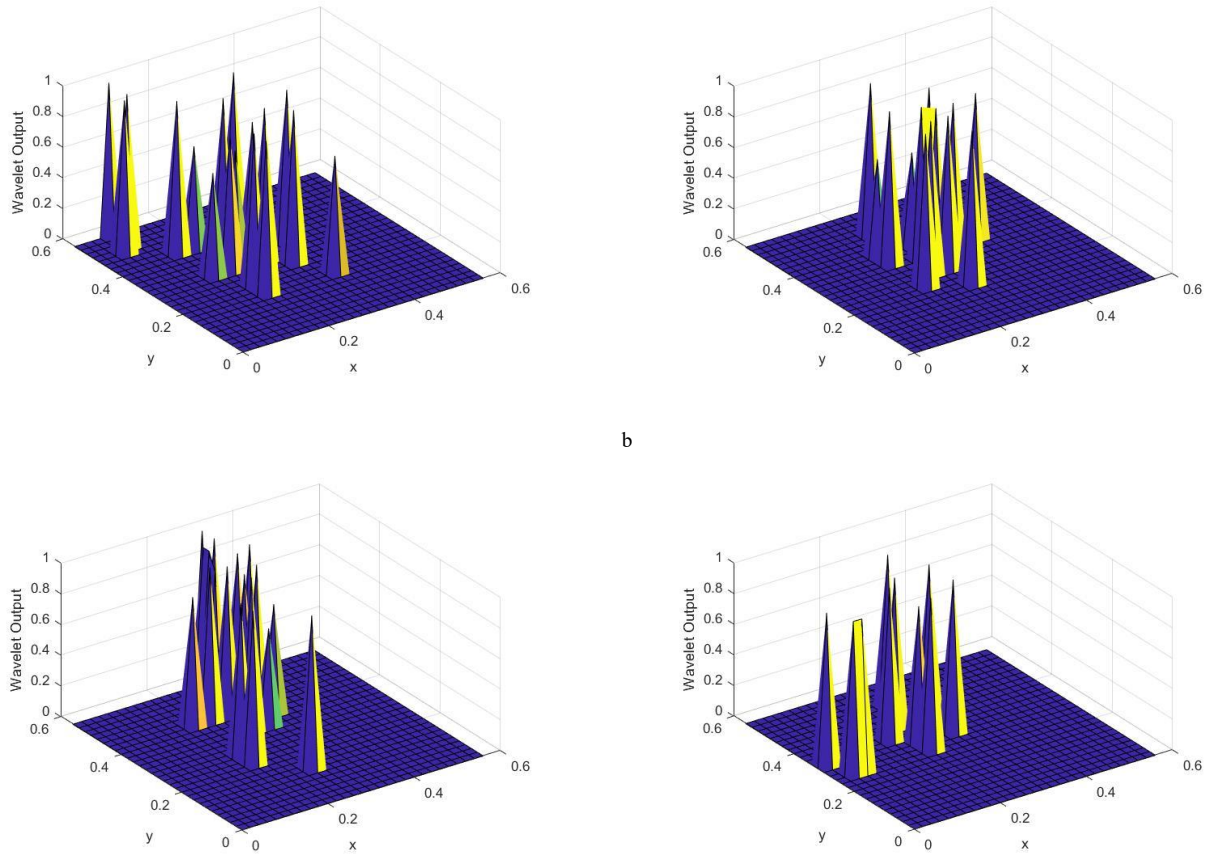

a b

c d

Figure 35. Damage localization results for scenarios a) first, b) second, c) third, and d) fourth with 50% damage severity in two-edge clamped plates using wavelet analysis with considering 3% noise

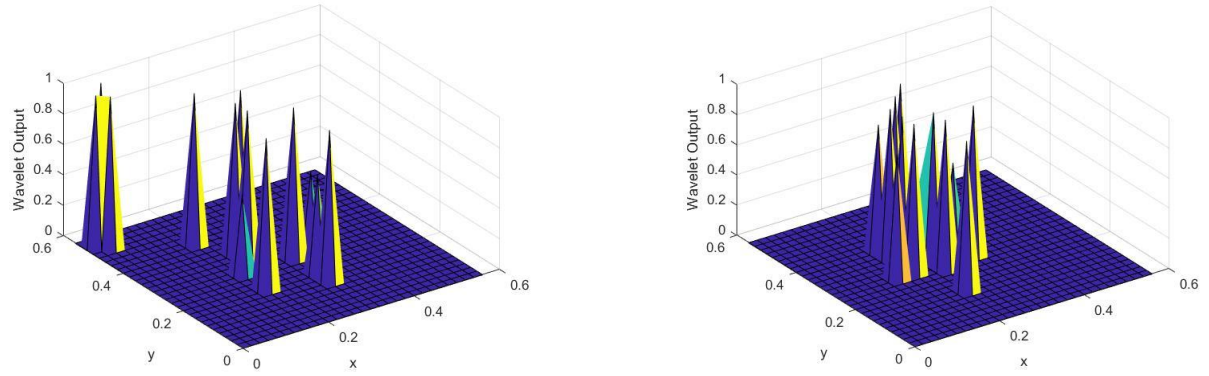

a b

Figure 36. Continued on next page

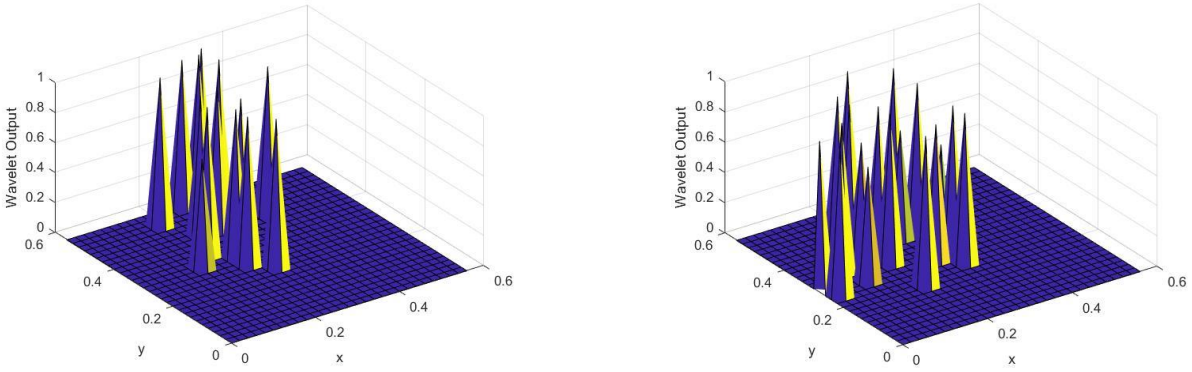

c d

Figure 36. Damage localization results for scenarios a) first, b) second, c) third, and d) fourth with 75% damage severity in two-edge clamped plates using wavelet analysis with considering 3% noise

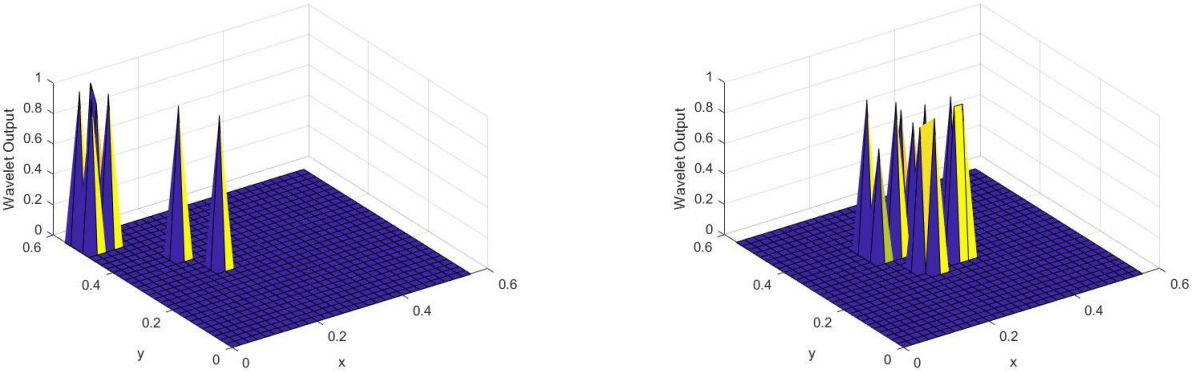

a b

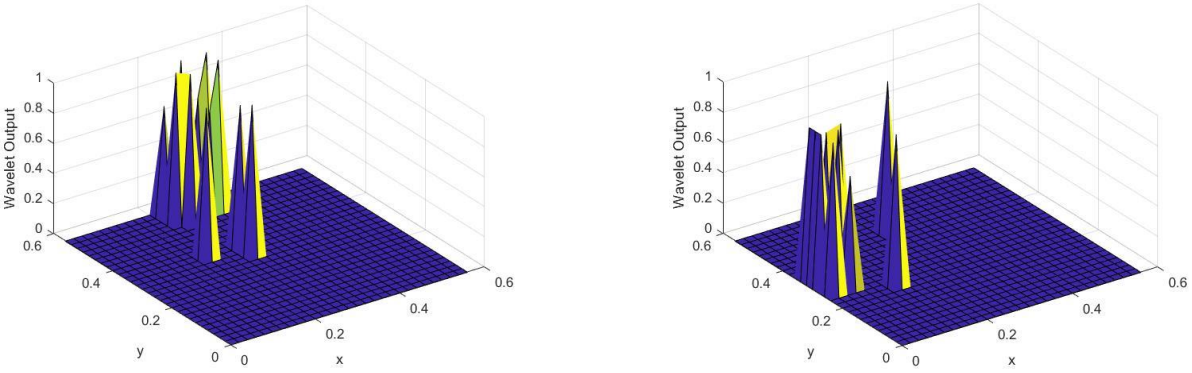

c d

Figure 37. Damage localization results for scenarios a) first, b) second, c) third, and d) fourth, with 87.5% damage severity in two-edge clamped plates using wavelet analysis with considering 3% noise

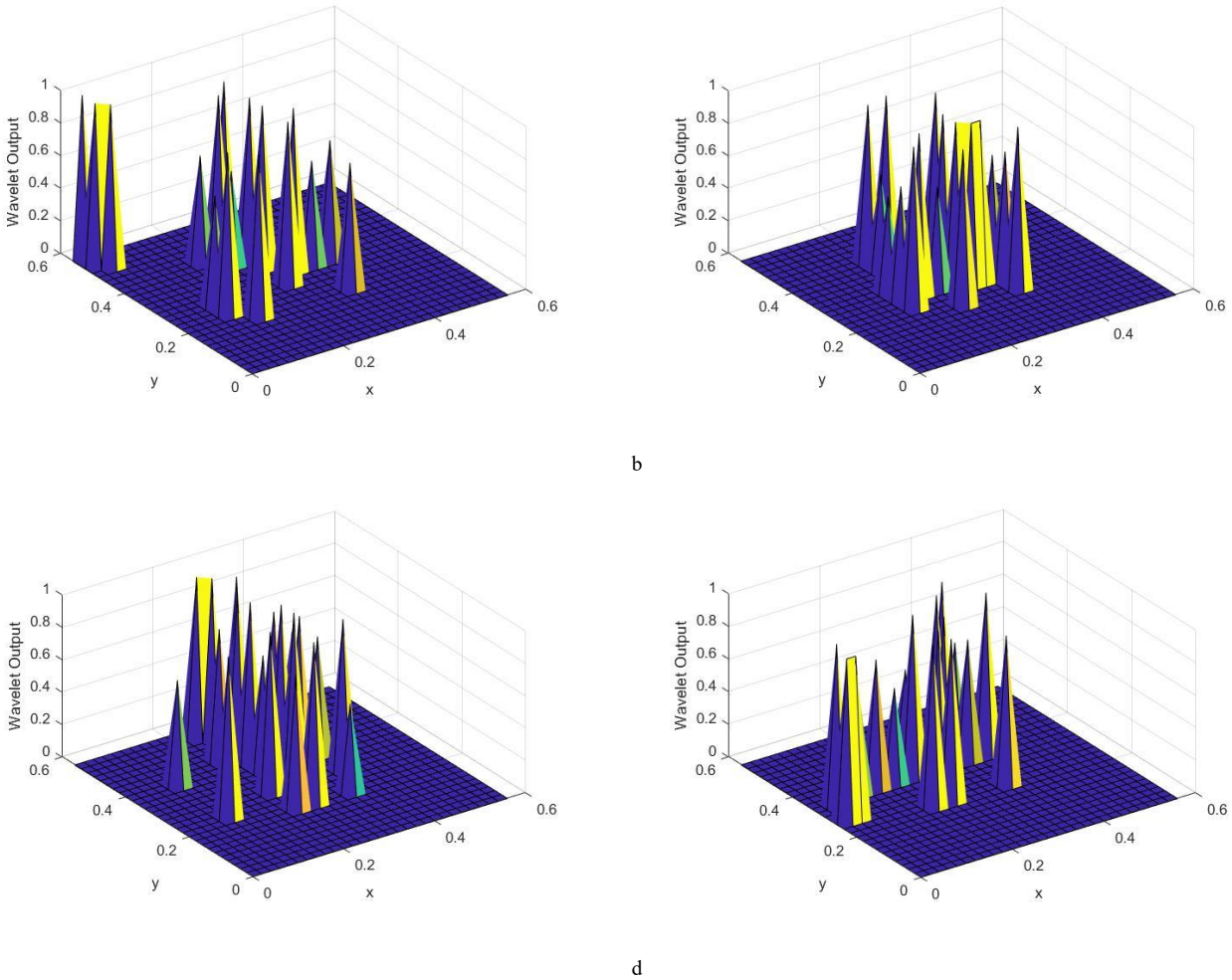

Figure 38. Damage localization results for scenarios a) first, b) second, c) third, and d) fourth with 25% damage severity in four-edge clamped plates using wavelet analysis with considering 3% noise

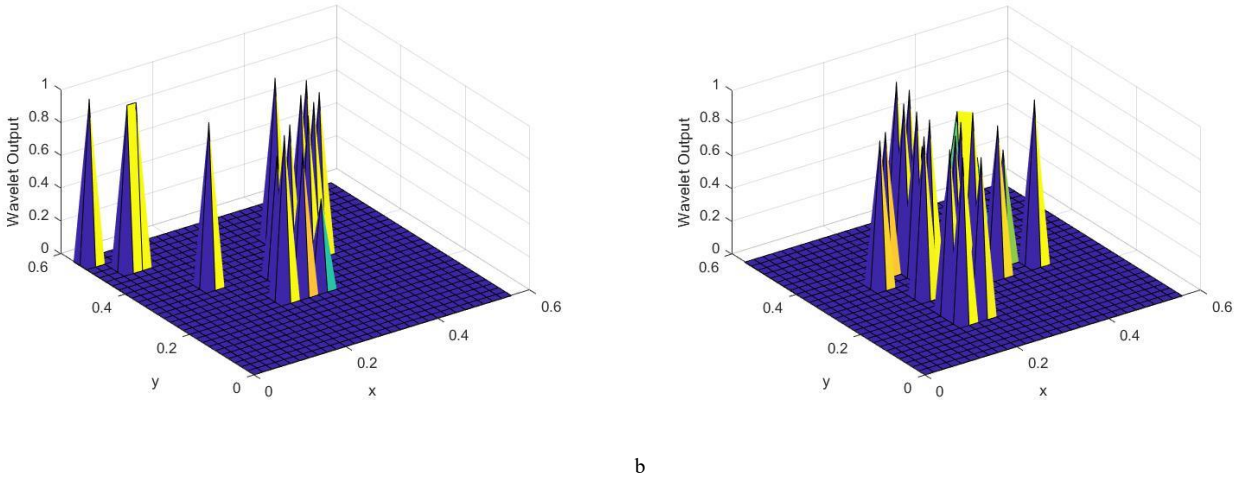

Figure 39. Continued on next page

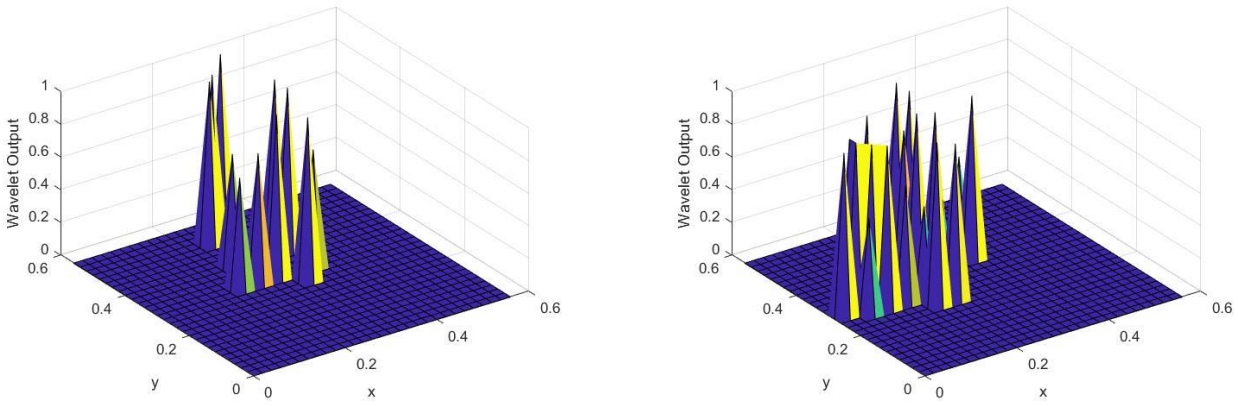

c d

Figure 39. Damage localization results for scenarios a) first, b) second, c) third, and d) fourth with 50% damage severity in four-edge clamped plates using wavelet analysis with considering 3% noise

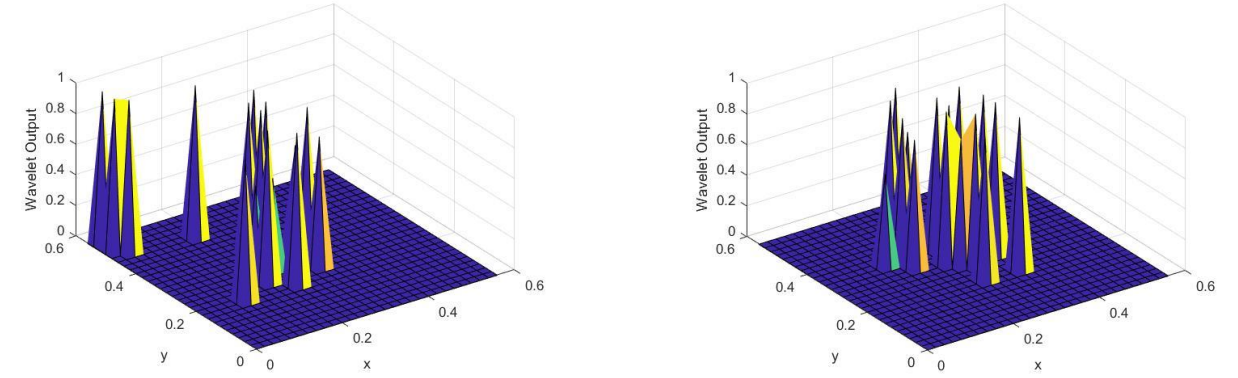

a b

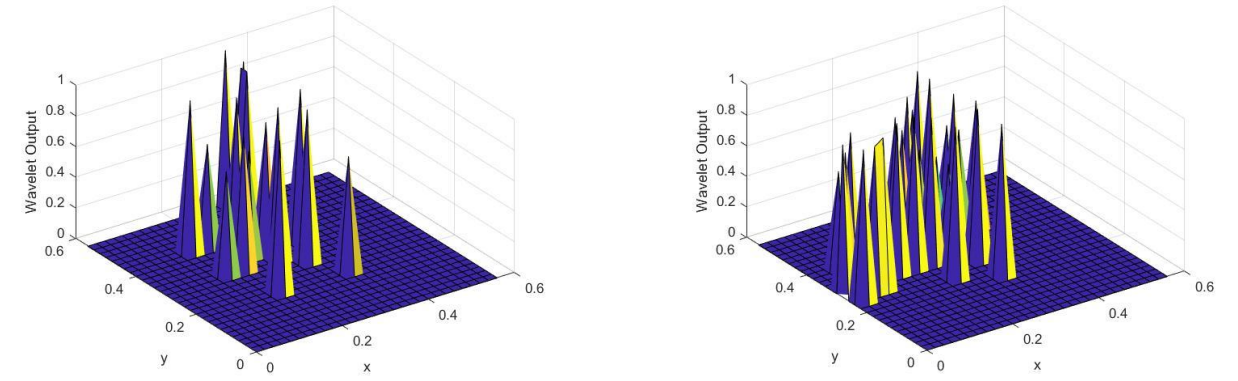

c d

Figure 40. Damage localization results for scenarios a) first, b) second, c) third, and d) fourth with 75% damage severity in four-edge clamped plates using wavelet analysis with considering 3% noise

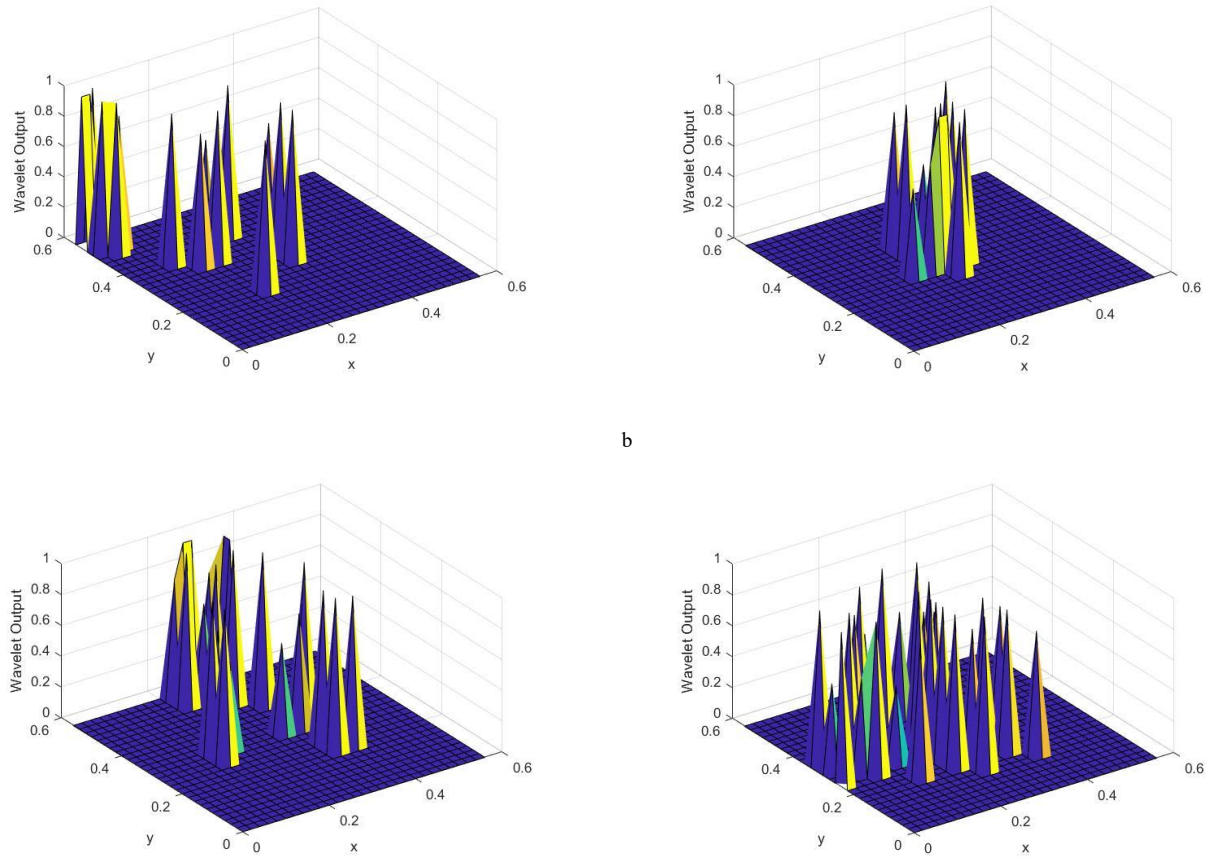

a b

c d

Figure 41. Damage localization results for scenarios a) first, b) second, c) third, and d) fourth, with 87.5% damage severity in four-edge clamped plates using wavelet analysis with considering 3% noise

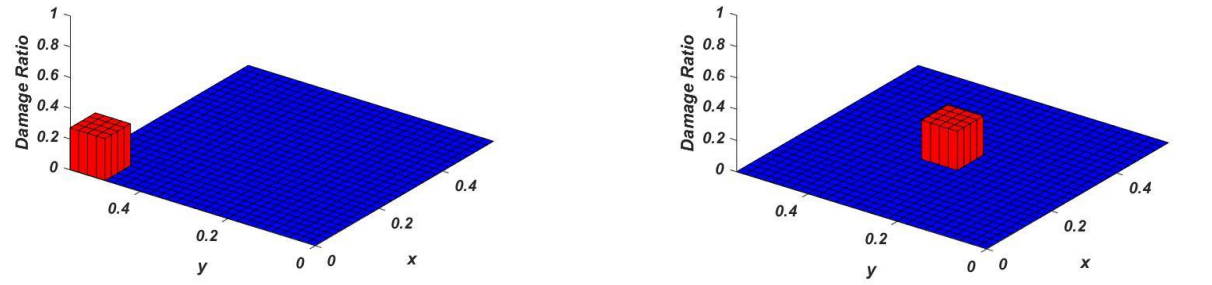

a b

Figure 42. Continued on next page

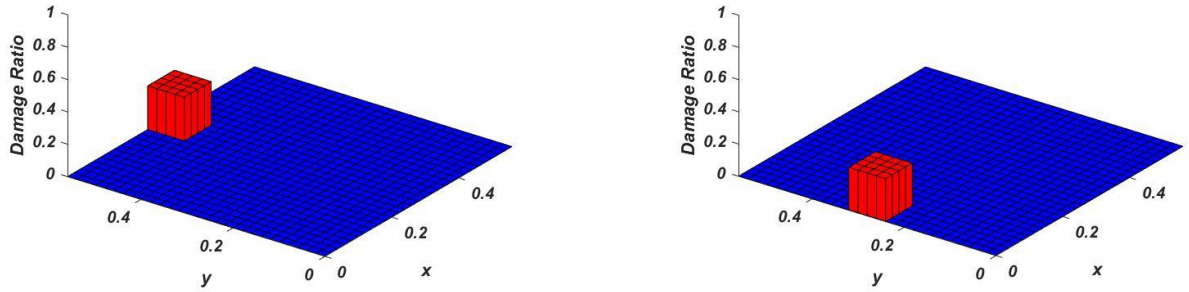

c d

Figure 42. Damage location and severity assessment for scenarios a) first, b) second, c) third, and d) fourth with 25% damage intensity in two-edge clamped plates without considering noise

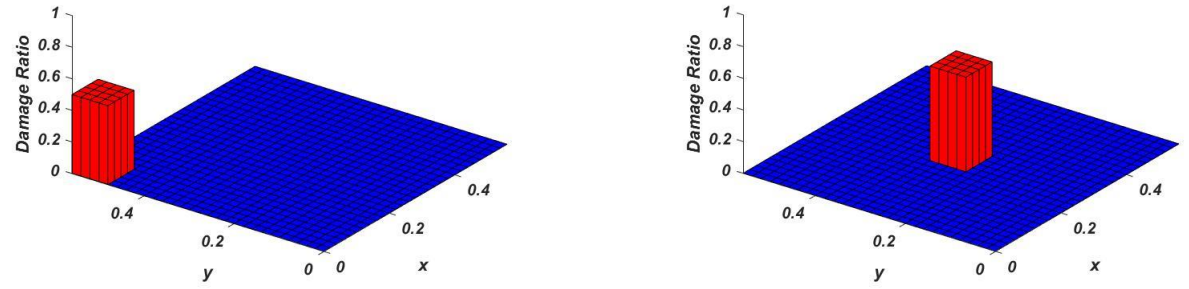

a b

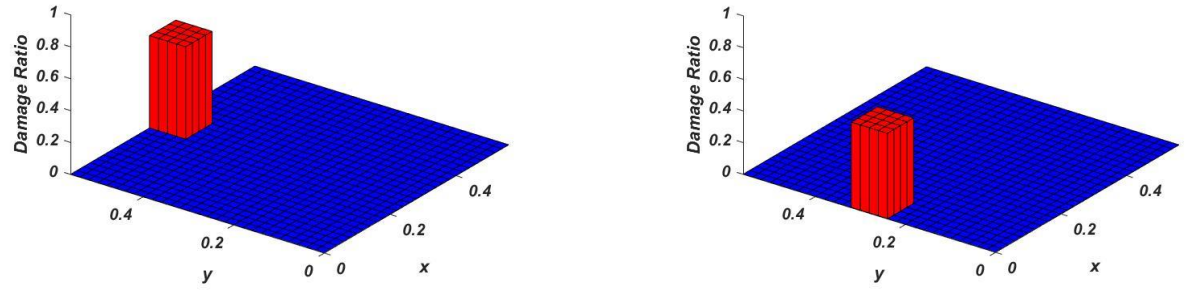

c d

Figure 43. Damage location and severity assessment for scenarios a) first, b) second, c) third, and d) fourth with 50% damage intensity in two-edge clamped plates without considering noise

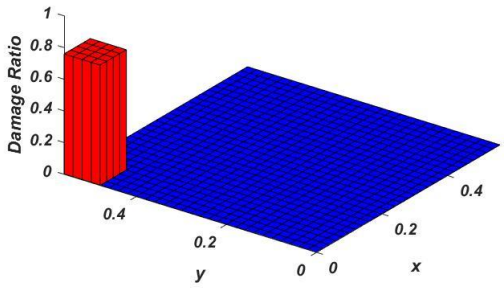

a

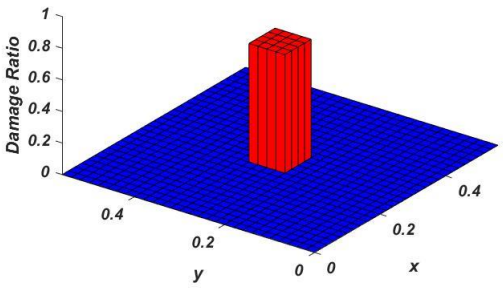

b

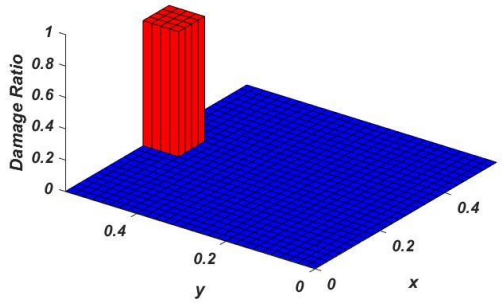

c

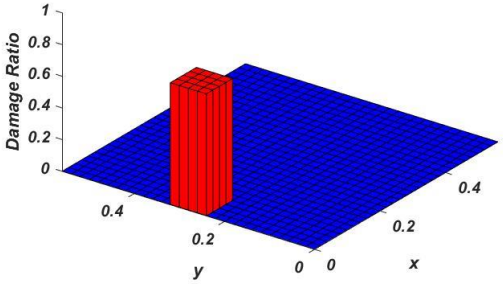

d

Figure 44. Damage location and severity assessment for scenarios a) first, b) second, c) third, and d) fourth with 75% damage intensity in two-edge clamped plates without considering noise

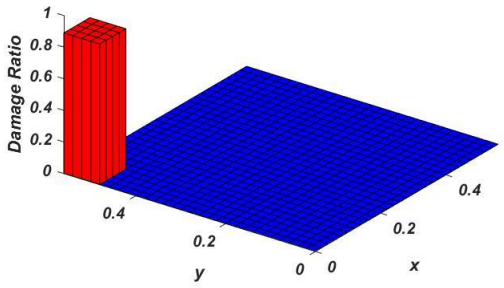

a

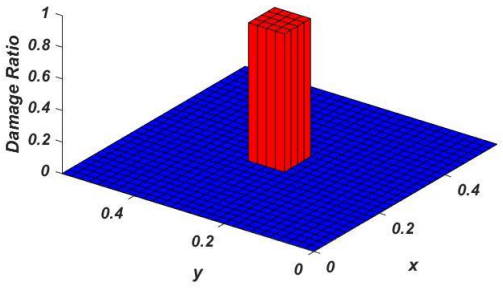

b

Figure 45. Continued on next page

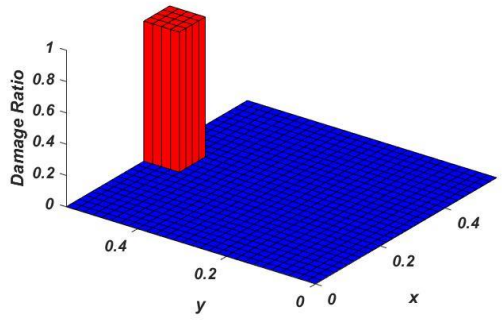

c

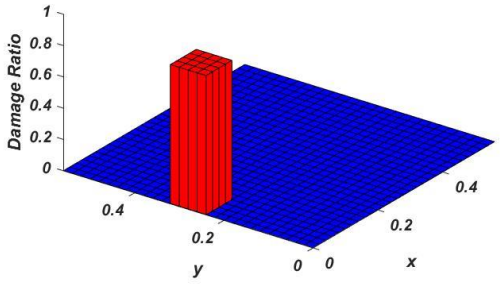

d

Figure 45. Damage location and severity assessment for scenarios a) first, b) second, c) third, and d) fourth, with 87.5% damage intensity in two-edge clamped plates without considering noise

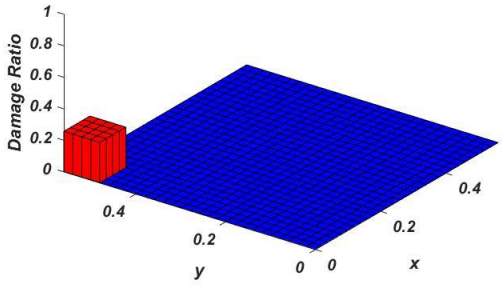

a

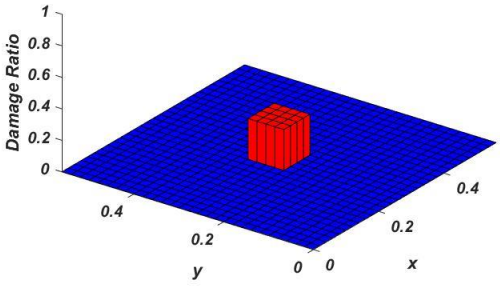

b

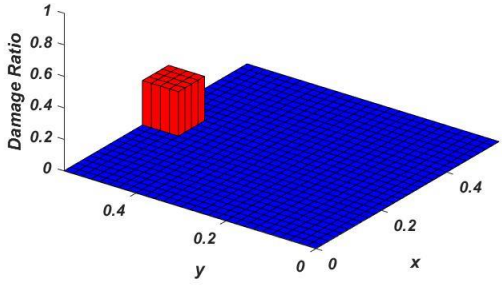

c

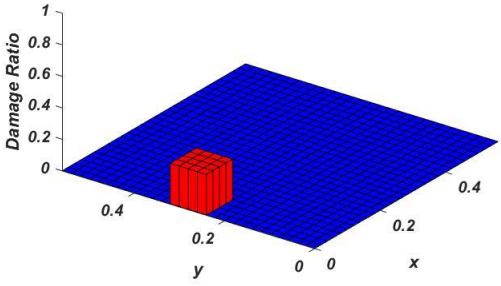

d

Figure 46. Damage location and severity assessment for scenarios a) first, b) second, c) third, and d) fourth with 25% damage intensity in four-edge clamped plates without considering noise

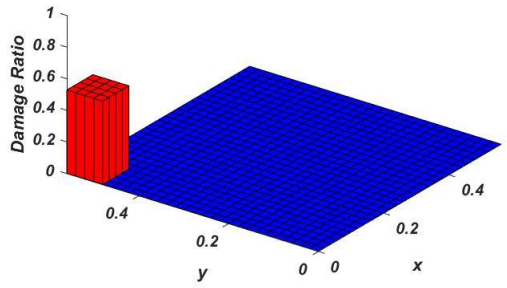

a

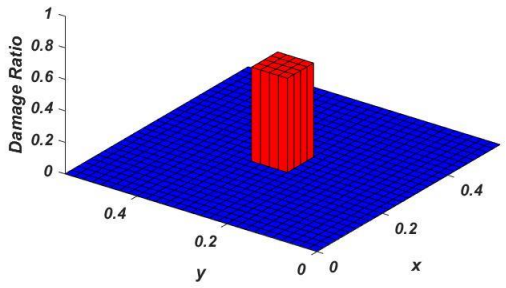

b

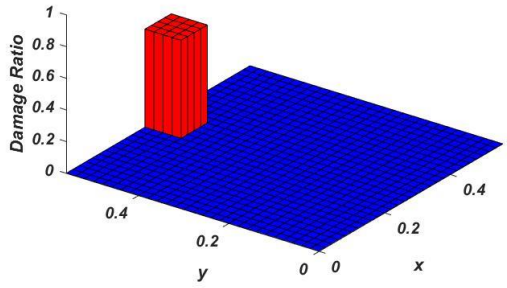

c

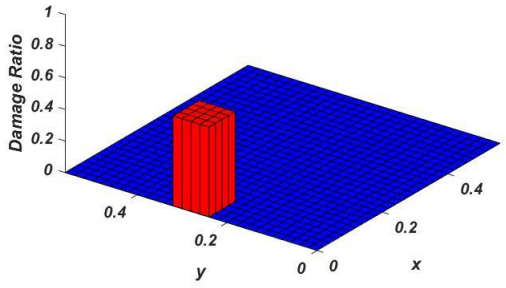

d

Figure 47. Damage location and severity assessment for scenarios a) first, b) second, c) third, and d) fourth with 50% damage intensity in four-edge clamped plates without considering noise

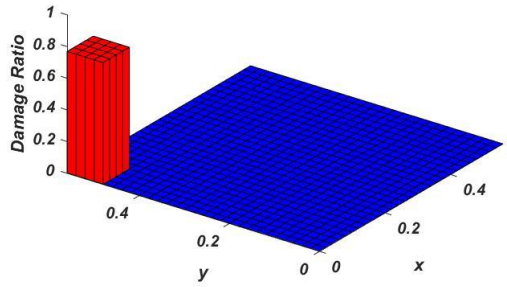

a

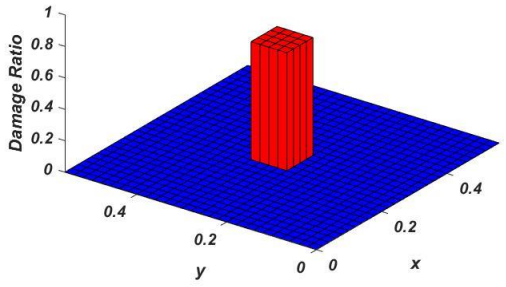

b

Figure 48. Continued on next page

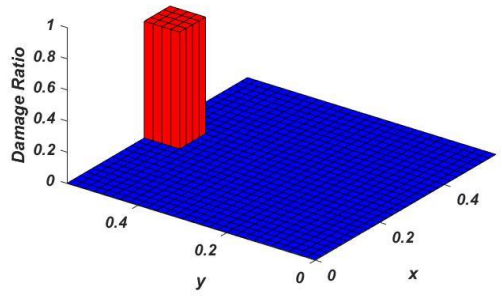

c

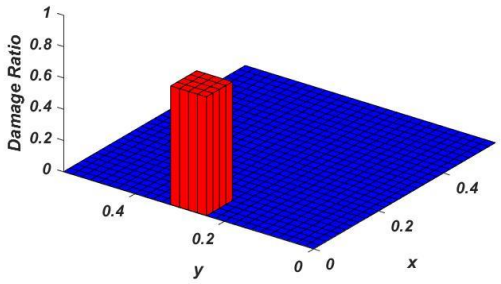

d

Figure 48. Damage location and severity assessment for scenarios a) first, b) second, c) third, and d) fourth with 75% damage intensity in four-edge clamped plates without considering noise

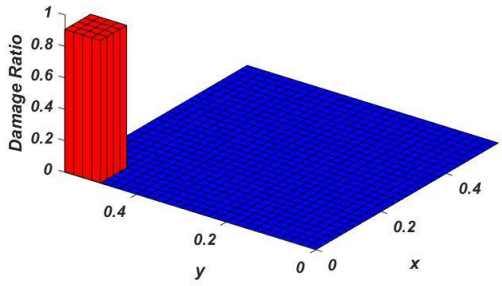

a

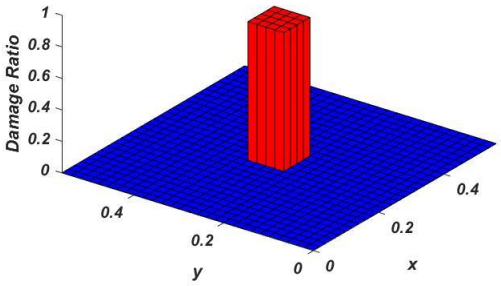

b

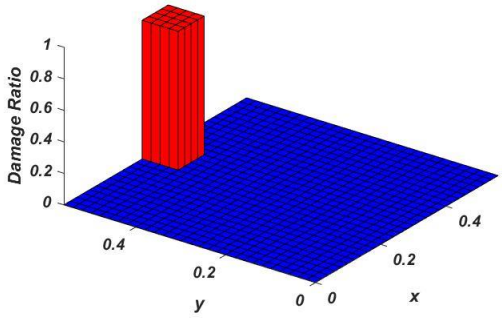

c

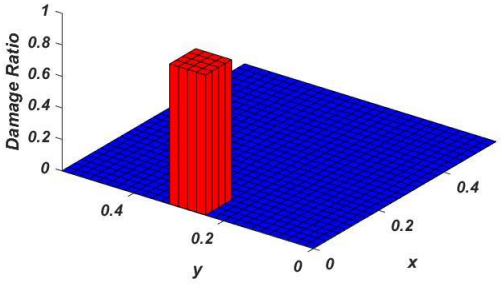

d

Figure 49. Damage location and severity assessment for scenarios a) first, b) second, c) third, and d) fourth, with 87.5% damage intensity in four-edge clamped plates without considering noise

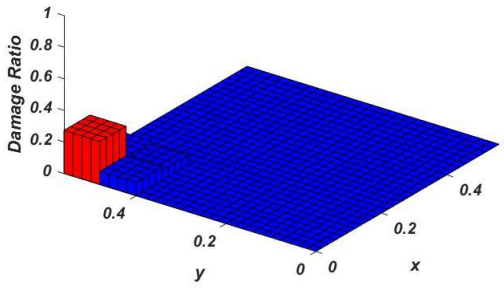

a

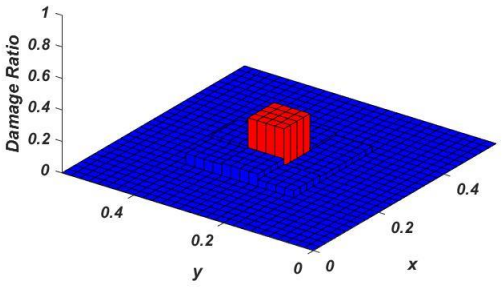

b

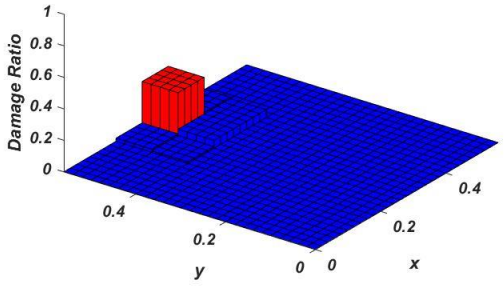

c

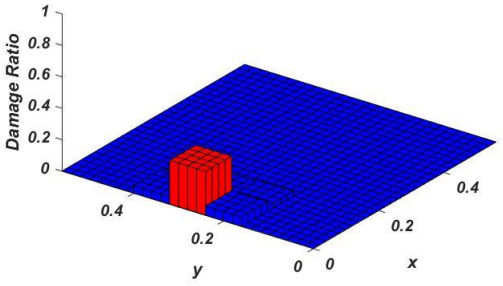

d

Figure 50. Damage location and severity assessment for scenarios a) first, b) second, c) third, and d) fourth with 25% damage intensity in two-edge clamped plates with considering 3% noise

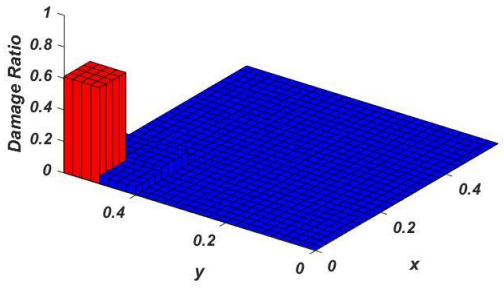

a

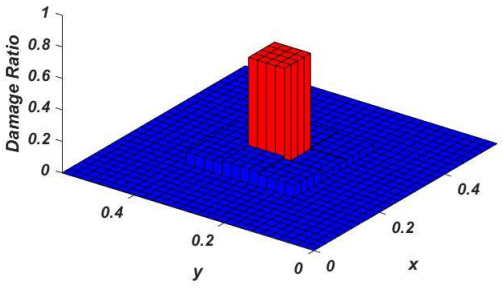

b

Figure 51. Continued on next page

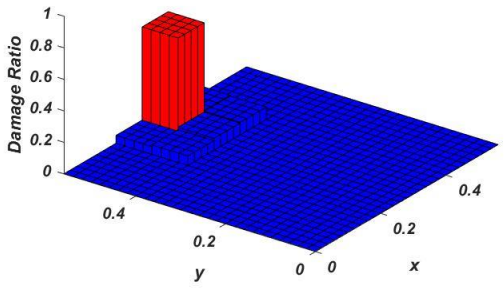

c

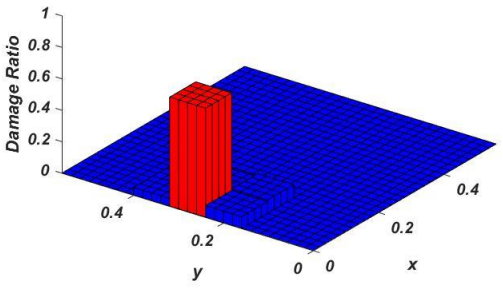

d

Figure 51. Damage location and severity assessment for scenarios a) first, b) second, c) third, and d) fourth with 50% damage intensity in two-edge clamped plates with considering 3% noise

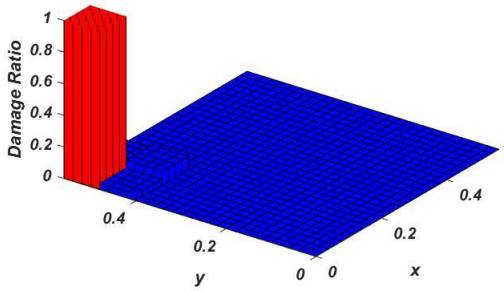

a

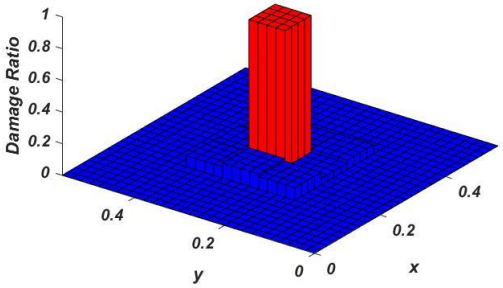

b

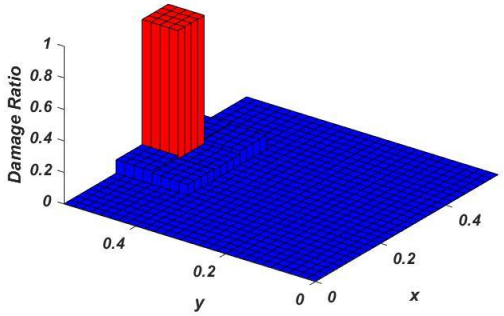

c

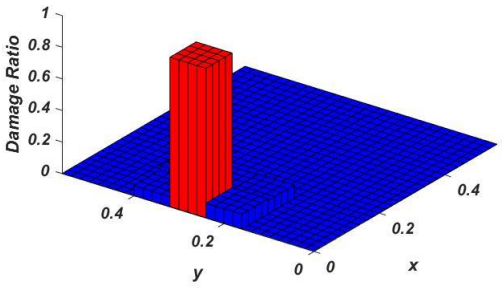

d

Figure 52. Damage location and severity assessment for scenarios a) first, b) second, c) third, and d) fourth with 75% damage intensity in two-edge clamped plates with considering 3% noise

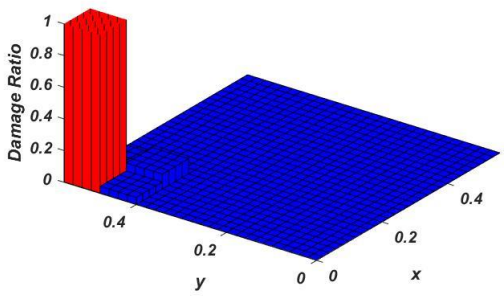

a

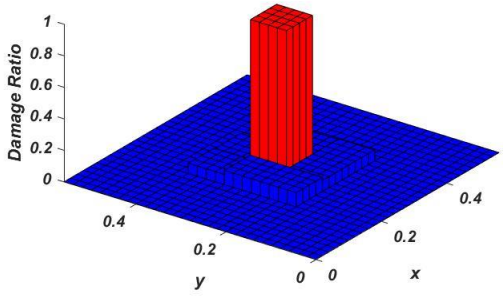

b

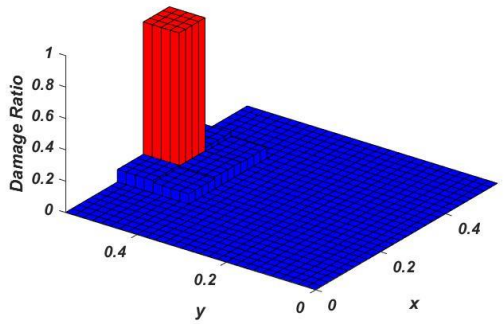

c

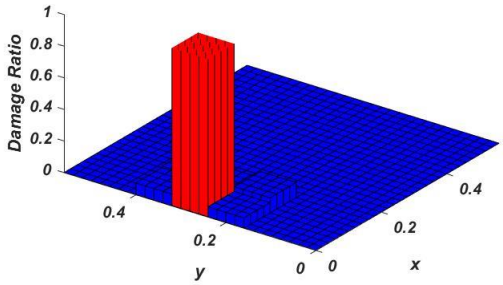

d

Figure 53. Damage location and severity assessment for scenarios a) first, b) second, c) third, and d) fourth, with 87.5% damage intensity in two-edge clamped plates with considering 3% noise

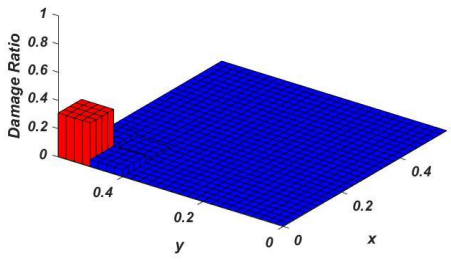

a

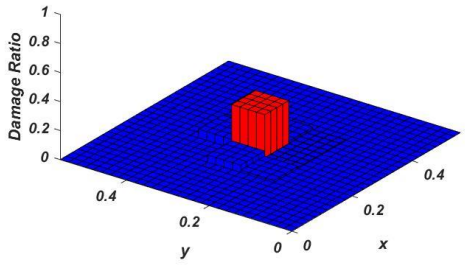

b

Figure 54. Continued on next page

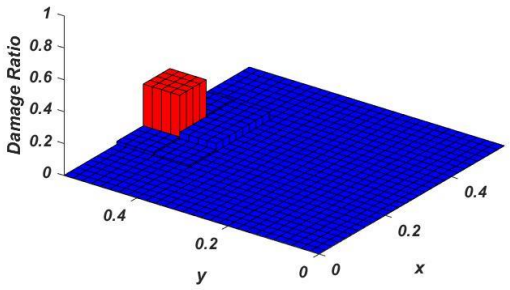

c

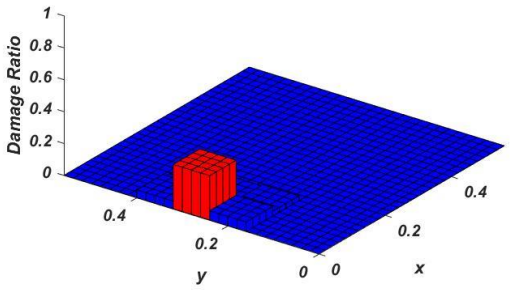

d

Figure 54. Damage location and severity assessment for scenarios a) first, b) second, c) third, and d) fourth with 25% damage intensity in four-edge clamped plates with considering 3% noise

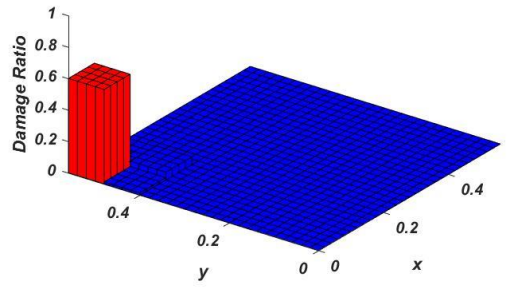

a

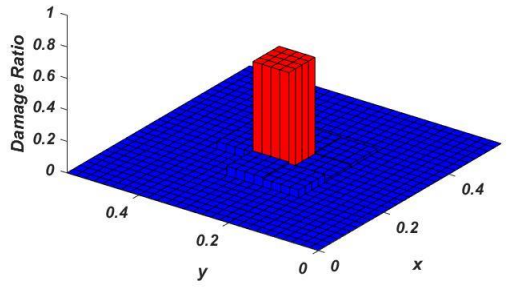

b

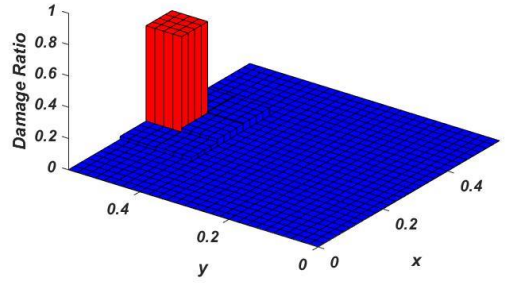

c

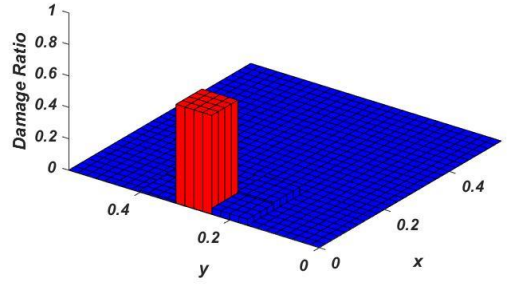

d

Figure 55. Damage location and severity assessment for scenarios a) first, b) second, c) third, and d) fourth with 50% damage intensity in four-edge clamped plates with considering 3% noise

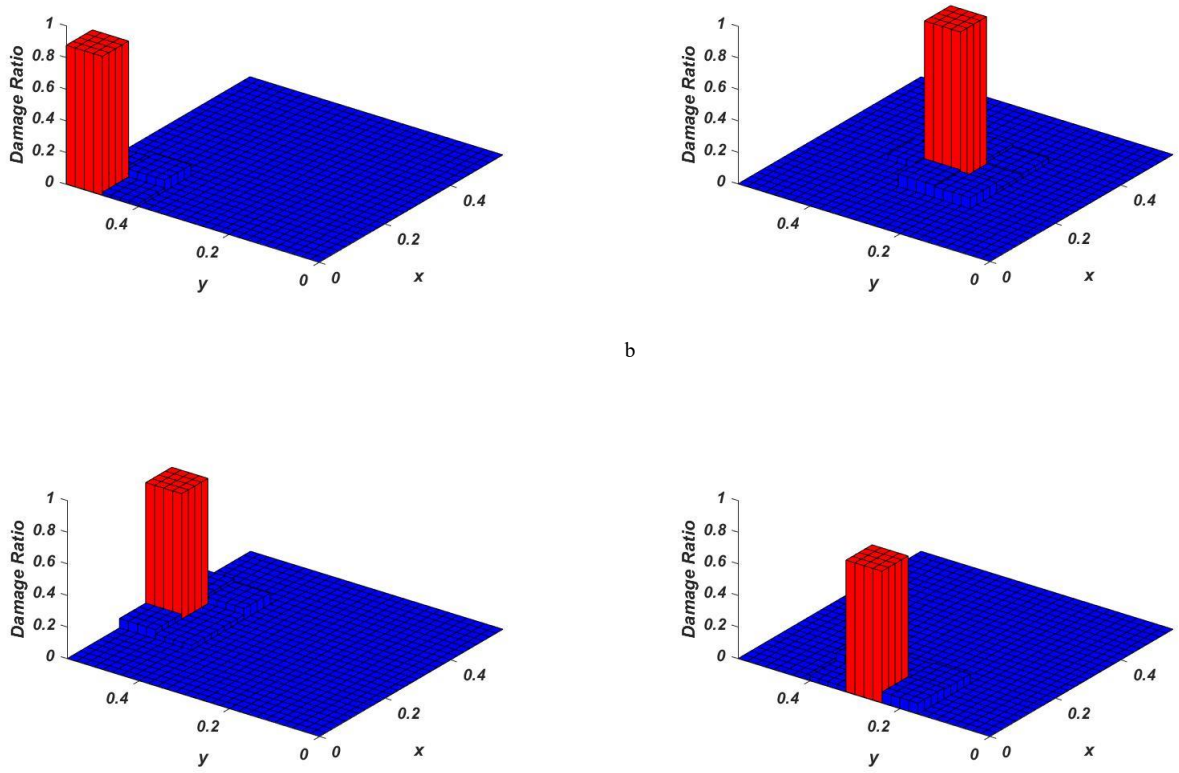

a b

c d

Figure 56. Damage location and severity assessment for scenarios a) first, b) second, c) third, and d) fourth with 75% damage intensity in four-edge clamped plates with considering 3% noise

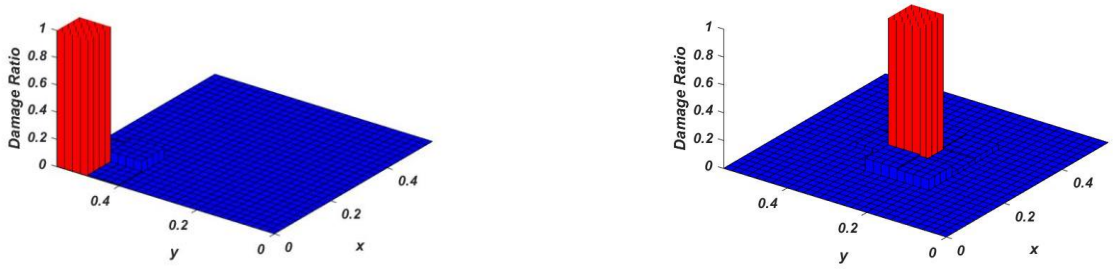

a b

Figure 57. Continued on next page

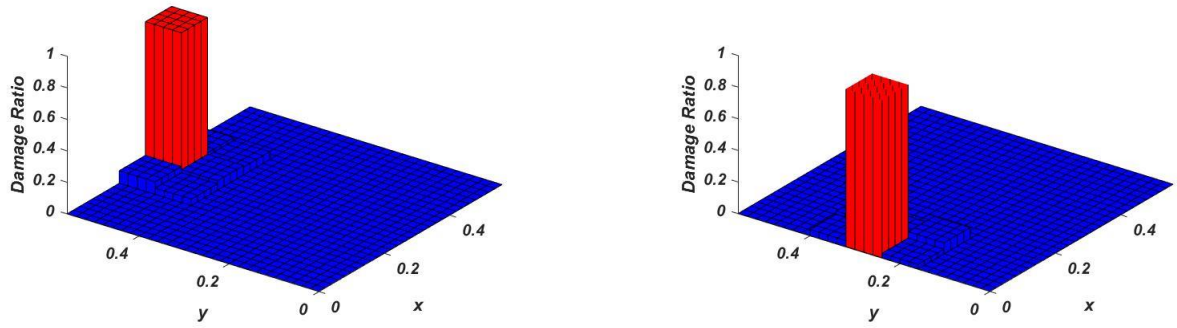

c d

Figure 57. Damage location and severity assessment for scenarios a) first, b) second, c) third, and d) fourth, with 87.5% damage intensity in four-edge clamped plates with considering 3% noise

In the 25% damage condition, with 3% noise application and in scenarios 1 to 4, damage intensity in simply supported plates on two sides is identified with differences of 8%, 9.29%, 136.94%, and 180.16%, respectively, while in plates fixed on four sides, the differences are 20%, 24.20%, 12%, and 12.72%, respectively. In the 50% damage condition, with 3% noise consideration and in scenarios 1 to 4, damage intensity in simply supported plates on two sides is identified with differences of 30.6%, 22.01%, 38.99%, and 28.20%, respectively, while in plates clamped on four sides, the differences are 25.37%, 20.49%, 26.06%, and 25.84%, respectively. In the 75% damage condition, with 3% noise consideration and in scenarios 1 to 4, damage intensity in simply supported plates on two sides was identified with differences of 20.45%, 77.48%, 26.34%, and 17.15%, respectively, while in plates clamped on four sides, the differences are 27.22%, 17.04%, 11.25%, and 9.71%, respectively. In the 87.5% damage condition, with 3% noise consideration and in scenarios 1 to 4, damage intensity in simply supported plates on two sides is identified with differences of 8.57%, 44.91%, 17.82%, and 5.53%, respectively, while in plates fixed on four sides, the differences are 26.07%, 19.15%, 51.61%, and 6.08%, respectively.

6. Conclusion

In this study, a damage identification method has been introduced using wavelet transforms and firefly optimization algorithm. In the first stage, the acceleration responses of structures obtained by utilizing a finite element analysis software have been subjected to wavelet transforms. Disturbances in response data indicate the presence of damage in the structure. Using filters, structural response signal details are extracted, and this principle leads to introducing a quantitative index for determining probable damage locations. In the second stage, the firefly optimization algorithm has been employed to accurately identify the damage location and severity. According to the results obtained from the beams with 16 and 27 elements, the wavelet index successfully identified damage location in both single and double damage cases. In the second step, slight differences have been observed, particularly in cases of double damage cases. In plate structures for both support conditions considered, during detection by the wavelet index, damaged locations have been identified within acceptable ranges, even with noise presence. In the case of plates clamped on four sides compared to two sides, more effective performance has been achieved in terms of damage intensity accuracy. Based on results, despite higher-level noise in the data, the suggested method has still provided the damage location and severity with rather high accuracy, which proves that the proposed method is very effective. Therefore, the results indicate that the method possesses good capability in identifying damage location and severity.

References

[1] Quek, S. T., Q. Wang, L. Zhang, and K.-K. Ang. "Sensitivity analysis of crack detection in beams by wavelet technique." International Journal of Mechanical Sciences 43.12 (2001): 2899-2910.

[2] Ovanesova, A. and L. E. Suarez. "Applications of wavelet transforms to damage detection in frame structures." Engineering Structures 26.1 (2004): 39-49.

[3] Loutridis, S., E. Douka, L. J. Hadjileontiadis, and A. Trochidis. "A two-dimensional wavelet transform for detection of cracks in plates." Engineering Structures 27.9 (2005): 1327-1338.

[4] Rucka, M. and K. Wilde. "Application of continuous wavelet transform in vibration based damage detection method for beams and plates." Journal of Sound and Vibration 297.3-5 (2006): 536-550. https://doi.org/10.1016/j.jsv.2006.04.020
[5] Xiang, J. and M. Liang. "A two-step approach to multi-damage detection for plate structures." Engineering Fracture Mechanics 91 (2012): 73-86. https://doi.org/10.1016/j.engfracmech.2012.04.027
[6] Hashem Jahangir and Mohammad Reza Esfahani. "Using wavelet transform of vibration modes for damage assessment of reinforced concrete beams." Fourth National Conference on Concrete of Iran, Tehran (2013).
[7] Ezzoldin, Amir, Hossein Naderpour, Ali Kheyroddin, and Gholamreza Ghodrati Amiri. "Crack location and magnitude detection in beams using wavelet transform." Modeling in Engineering 12.39 (2014): 89-99.
[8] Hajizadeh, A., E. Salajegheh, and J. Salajegheh. "2–d discrete wavelet–based crack detection using static and dynamic responses in plate structures." Asian Journal of Civil Engineering 17.6 (2016): 713-735.
[9] Ahmadi, Mohtasham Khan, Omid Rezaei Far, and Majid Gholhaki. "Fault detection in steel beams using comparison of continuous wavelet transform analytical results of primary and secondary mode shapes." Third International Conference on Applied Research in Structural Engineering and Construction Management, Tehran (2019).
[10] Guo, J., D. Guan, and J. Zhao. "Structural damage identification based on the wavelet transform and improved particle swarm optimization algorithm." Advances in Civil Engineering 2020 (2020): 8869810. https://doi.org/10.1155/2020/8869810
[11] Luo, Y., L. Wang, X. Guo, J. Zheng, F. Liao, and Z. Guo. "Structural Damage Identification Based on Convolutional Neural Network Group Considering the Sensor Fault." KSCE Journal of Civil Engineering 27.8 (2023): 3403-3417. https://doi.org/10.1007/s12205-023-2070-0
[12] Abdushkour, H. A., M. Saadatmorad, S. Khatir, B. Benaissa, F. Al Thobiani, and A. U. Khawaja. "Structural Damage Detection by Derivative-Based Wavelet Transforms." Arabian Journal for Science and Engineering 49.11 (2024): 15701-15709. https://doi.org/10.1007/s13369-024-09289-8
[13] Zhao, J., Z. Zhou, D. Guan, and L. Gong. "Structural edge damage detection based on wavelet transform and immune genetic algorithm." Scientific Reports 15.1 (2025): 4376. https://doi.org/10.1038/s41598-025-88974-4
[14] Sinha, J. K., M. Friswell, and S. Edwards. "Simplified models for the location of cracks in beam structures using measured vibration data." Journal of Sound and Vibration 251.1 (2002): 13-38. https://doi.org/10.1006/jsvi.2001.3988
[15] Yazdanpanah, O. and S. Seyedpoor. "A new damage detection indicator for beams based on mode shape data." Structural Engineering and Mechanics 53.4 (2015): 725-744. https://doi.org/10.12989/sem.2015.53.4.725
[16] Abdulkareem, M., N. Bakhary, M. Vafaei, N. M. Noor, and R. N. Mohamed. "Application of two-dimensional wavelet transform to detect damage in steel plate structures." Measurement 146 (2019): 912-923. https://doi.org/10.1016/j.measurement.2019.07.017
[17] Sadowsky, J. "Investigation of signal characteristics using the continuous wavelet transform." Johns Hopkins APL Technical Digest 17.3 (1996): 258-269.
[18] Jordan, D., R. Miksad, and E. Powers. "Implementation of the continuous wavelet transform for digital time series analysis." Review of Scientific Instruments 68.3 (1997): 1484-1494. https://doi.org/10.1063/1.1147636
[19] Yang, X. S. "Firefly algorithm, Levy flights and global optimization." In Research and Development in Intelligent Systems XXVI, Springer (2010): 209-218. https://doi.org/10.1007/978-1-84882-983-1_15